NOAA Technical Memorandum ERL PMEL-42

DATA INTERCOMPARISON THEORY

V. CASE STUDY: EFFECTS OF OBJECTIVE ANALYSIS ON A TROPICAL PACIFIC SEA SURFACE TEMPERATURE SET

Rudolph W. Preisendorfer
Curtis D. Mobley

Pacific Marine Environmental Laboratory
Seattle, Washington
December 1982

UNITED STATES DEPARTMENT OF COMMERCE
Malcolm Baldrige, Secretary

NATIONAL OCEANIC AND ATMOSPHERIC ADMINISTRATION
John V. Byrne, Administrator

Environmental Research Laboratories
George H. Ludwig Director

NOTICE

Mention of a commercial company or product does not constitute an endorsement by NOAA Environmental Research Laboratories. Use for publicity or advertising purposes of information from this publication concerning proprietary products or the tests of such products is not authorized.

Contribution No. 604 from NOAA's Pacific Marine Environmental Laboratory

TABLE OF CONTENTS

Abstract

A study is made of an objective analysis scheme by Liu which has SST-gradient-dependent smoothing and correction operations, along with data-weight and outlier cutoff features. The scheme is an elaboration of that originally devised by Cressman and subsequently expanded by Levitus and Oort. The object of the study is to apply certain new data intercomparison techniques (developed in the four earlier works of the present series) to the data set produced by Liu's scheme, with the goal in mind to determine how the various features of the new objective analysis scheme change the location (average), scale (variance), and pattern properties of the data set. In general it is found that the *average* properties of a data set are largely unchanged by application of the above features of Liu's scheme. However, the *variance* and *pattern* properties are significantly changed by the various smoothing operations in Cressman-type objective analysis schemes. In the case of Liu's data set the changes are by amounts (0.5°C) that are climatologically important. Thus a new objective analysis scheme may *significantly* affect location, scale and pattern properties of a data set, and therefore in ways that could affect the formation and verification of hypotheses of climatic change.

Data Intercomparison Theory

V. Case Study: Effects of Objective Analysis on a Tropical Pacific Sea Surface Temperature Set

Rudolph W. Preisendorfer

Curtis D. Mobley

1. Introduction

In this study, the fifth and final of the present series on data intercomparison theory, we apply the tests developed in the preceding works to a Pacific tropical sea surface temperature data set devised by Liu (1982). The screened data of this set have been assembled from various sources and skillfully combined by Liu using a new objective analysis scheme (see Appendix A). The several new features incorporated in the scheme, such as weighting data according to source, outlier cutoff, and, finally, correcting and smoothing data, afford the opportunity to apply the above intercomparison tests, under realistic conditions, to a data set that has great potential for subsequent applications. Specifically we intend first to remove the SST-gradient-sensitive feature and the data-weight feature of Liu's scheme to produce a new set which we will then compare with Liu's in various ways. For example, we will see if there are significant changes in the main attributes of the sets, such as the average and variance properties, as well as spatial patterns and temporal evolutions. We will then produce a second new set by removing all novel features from Liu's scheme, thereby reducing it to a form devised originally by Levitus and Oort (1977) which in turn is an elaboration of the Cressman (1959) scheme. These three resultant sets ("Liu", "modified Levitus-Oort", "original Levitus-Oort") are then systematically intercompared

for significant differences of their various attributes. We shall find that there were significant differences introduced in the *variances* between data sets by Liu's novel smoothing operations. However, there were no significant changes in the *average* SST values of the data sets induced by the smoothing operations over the common domain of the sets. The variance differences induced by the smoothing operations are on the order of 0.5°C, a climatologically important magnitude. Finally, we found that turning off and turning on the SST-gradient-sensitive features in Liu's scheme does not produce *significantly* different sets in any sense (location, spread, or pattern) in high data-density high-gradient areas.

In sum, the various intercomparison tests developed in this series form a general set of procedures whereby the consequences of different objective analysis schemes, applied to a common data set, can be weighed for statistical significance.

Acknowledgments

We are indebted to Dr. Cho-Teng Liu for access to his data set prior to publication and also for producing special computations, using his objective analysis scheme, required for the present study. Dr. Liu's work, as well as Dr. Mobley's, were supported through grants from NOAA's Equatorial Pacific Ocean Climate Studies (EPOCS) program. Lai Lu and Ryan Whitney typed successive drafts of the manuscript, and Gini May and Joy Godfrey drew the figures. Editor Jean Chatfield's cooperation in expediting this lengthy series of studies during the typing stage is gratefully acknowledged.

2. Structure of the Liu, Modified Levitus-Oort, and Original Levitus-Oort Data Sets

In Liu (1982) there is a description of an objective analysis scheme for producing a tropical Pacific sea surface temperature set. The temperature data set in its final form consists of 144 contoured maps, extending from January 1975 through December 1980, at ½ month intervals, of the SST patterns over the Pacific between 25°N to 30°S and from the western coastline of the Americas to 150°E. Fig. 2.1 is a facsimile of the first of these maps (7501-1 = 1^{st} ½ month of January 1975) along with the locations of ships, XBT's, AXBT's and buoys, during the associated ½ month period, which supplied data for the map. The contours are spaced 1°C apart. The climatological mean over this region is about 25°C. The data, prior to objective analysis, were subjected to screening for the proper location of the data points (in the area of interest), proper temperature ranges (10°C to 35°C), climatology bounds (location- and season-dependent limits on readings), ship speed limits (data rejected if ship speeds above 14 m/sec were deduced from the records), proper air temperature (SST accepted if within 5°C of air temperature and not exactly equal to temperature of overlying air), and, finally, for redundant records (about 5% were culled out).

Once the data were screened, they were subject to a sequence of five operations which are named in the left column of Table 2.1. The mathematical forms of these operations are given in (A17.1)-(A17.5) of Appendix A. Since some knowledge of these operations is required for an appreciation of the intercomparison activities below, the reader may wish to peruse Appendix A before proceeding on to §3. For the moment we can define the three data sets to be intercompared, for the most part, in general terms, using Table 2.1.

LIU SST DATA SET

FIRST 1/2 MONTH PERIOD JANUARY 1975

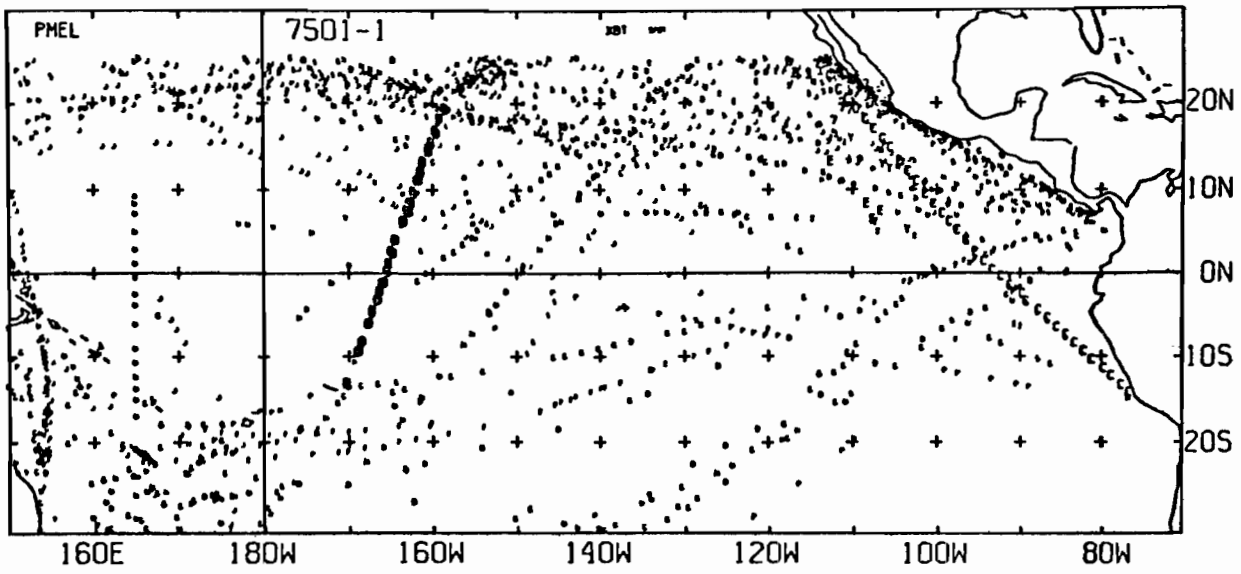

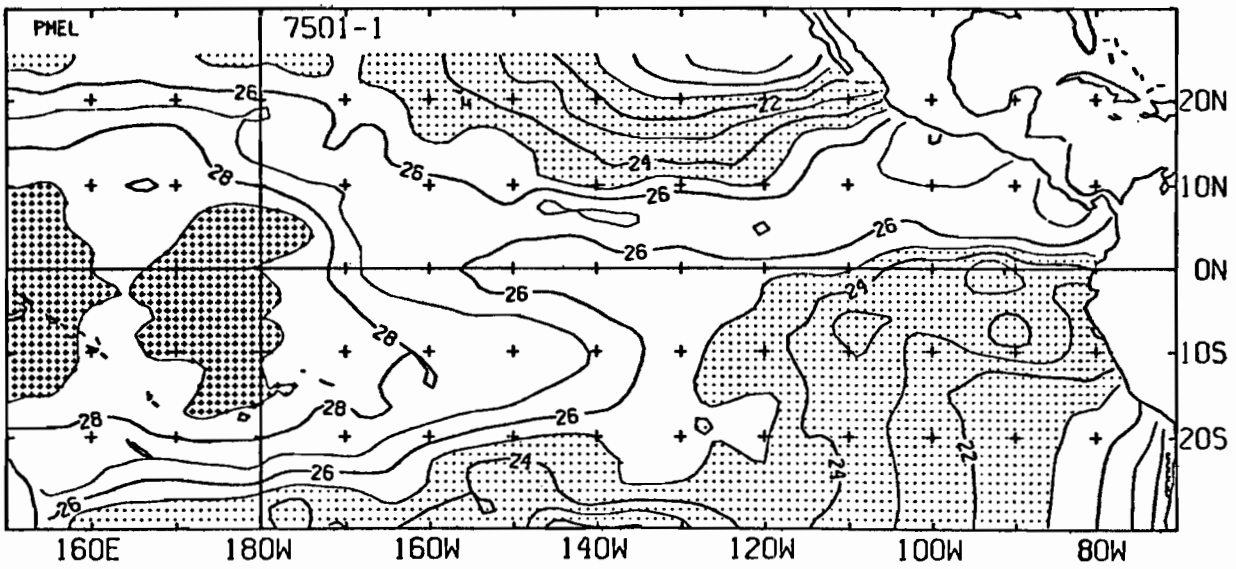

7501-1 SST. 0 E-BUØY. 0 BT. 102 XBT. 1568 SPØT DATA

Fig. 2.1

Table 2.1

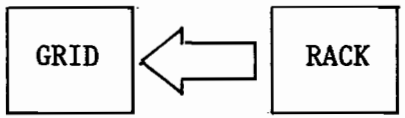

OBJECTIVE ANALYSIS SCHEMES

BASIC OPERATIONS ON SCREENED DATA	ORIG. LEV-ORT	MODF. LEV.-ORT	LIU
GRID TO RACK INTER-POLATOR	YES	YES	YES
CORRECTOR ON GRID	SST GRADIENT INDEPEND NO OUTLIER CUTOFF NO DATA WGT	SST GRADIENT INDEPEND OUTLIER CUTOFF NO DATA WGT	SST GRADIENT DEPEND OUTLIER CUTOFF DATA WGT
DIFFUSER-SMOOTHER	NO	SST GRADIENT INDEPEND	SST GRADIENT DEPEND
UPDATER	YES	YES	YES
CURVATURE-CORRECTOR	NO	YES	YES
LAPLACIAN-SMOOTHER	YES	YES	YES

The Liu objective analysis scheme starts with an interpolation of a given climatological SST set defined on a 1°×1° grid. This interpolation maps from the grid onto points of the rack - i.e., the stations over the sea surface where data are given (see upper panel in Fig. 2.1 for the rack going with 1st ½ of January 1975). The second step in Liu's scheme is a correction operation for the grid data, defined by the discrepancy existing between the data field on the rack and the interpolated field from grid to rack. Liu, in this step, has made the correction dependent on the local SST gradient of the screened data set. Moreover, he has assigned weights to the data values in accordance with the conventions in (A12.1). Finally, still in the correcter-on-grid operation, there is an outlier cutoff with cutoff values as defined in (A17.6). In the third operation, there is again an SST gradient-dependent diffuser-smoother activity. The above correction and the result of the diffuser-smoothing are then used to update the grid field. Liu adds a curvature-corrector step and then ends up with a Laplacian-smoother operation. In all, this set of five steps is gone through seven times with gradient-sensing and cutoff limits varying from one iteration to another, as shown in (A17.6). The final field $d'(i,j)$ on the 1°×1° grid is given by (A17.7).

The modified Levitus-Oort scheme is obtained from Liu's as shown in the middle column of Table 2.1. There, it is seen we have dropped the data-weight and SST-gradient-dependent features. We asked Liu, in the operation of the diffuser-smoother and the corrector, to set $f_a \equiv 1$, $f_c \equiv 1$, and $R_x(i,j) = R_y(i,j) = 2b^{(r)}$, where $b^{(r)} = 3$, or 4, according to (A17.6). The outlier cutoff feature was retained. For economic reasons we limited the production of the resultant set to the period January 1975 - June 1976 over a 2°×2° subgrid of the 1°×1° grid. The result is called the "modified Levitus-Oort" SST data set.

After a preliminary intercomparison of the Liu and modified Levitus-Oort sets, over the common 2°×2° grid, which showed them to be not significantly different in several attributes (to be described below), we asked Liu to drop in addition several other features of his scheme, namely the outlier cutoff, the diffuser-smoother and the curvature corrector. The resultant operations are shown in the first column of Table 2.1, and these yielded what we called the "original Levitus-Oort" data set over the period January 1975 - June 1976, on a 2°×2° grid.

The data-data intercomparisons and analyses below therefore take place on a common 2°×2° grid over the time period January 1975 - June 1976, unless otherwise stated. A sample map from the modified Levitus-Oort field is shown in Fig. 2.2 and one from the original Levitus-Oort field is shown in Fig. 2.3. The contour lines are spaced 1°C apart, just as in Fig. 2.1. In Figure 2.3 the absence of the effects of the diffuser-smoother is most noticeable. On comparing Figs. 2.1, 2.2, 2.3, several questions come to mind. Is the average of the field in Fig. 2.3 significantly different from that of the Liu set in Fig. 2.1? The spatial variance seems to be higher in the original Levitus-Oort set of Fig. 2.3 relative to the Liu set. But what about temporal variance: is it more than we might attribute to chance, in view of the known behavior of the SST field over the 18 month period January 1975 - June 1976? Are the temporal changes significantly different among the data sets? Are there regions over the common domain of these data sets where the resemblances in spatial pattern or temporal evolution among the three pairs of sets are significantly different? What role does the new gradient-sensitive feature of Liu's scheme play in forming his resultant data set? What role does data density play in the resultant data field over data sparse and data rich regions? What role is there for the diffuser-smoother and curvature-corrector

MODIFIED 'LEVITUS-OORT' SST DATA SET
1ST 1/2 MONTH PERIOD, JAN 75

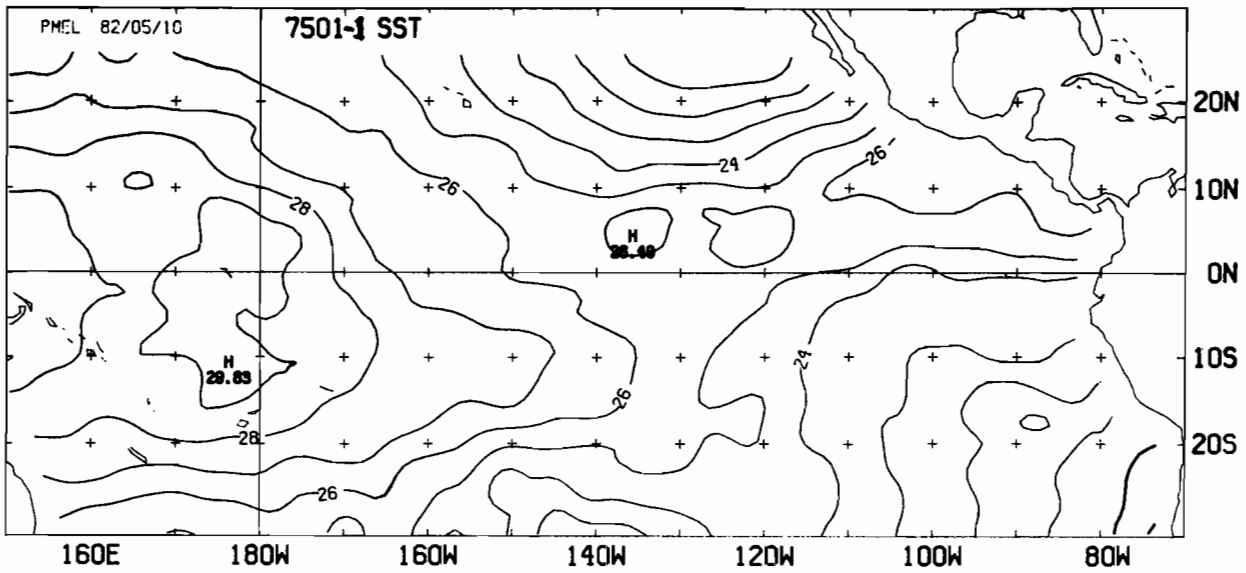

ORIGINAL 'LEVITUS-OORT' SST DATA SET
1ST 1/2 MONTH PERIOD, JAN 75

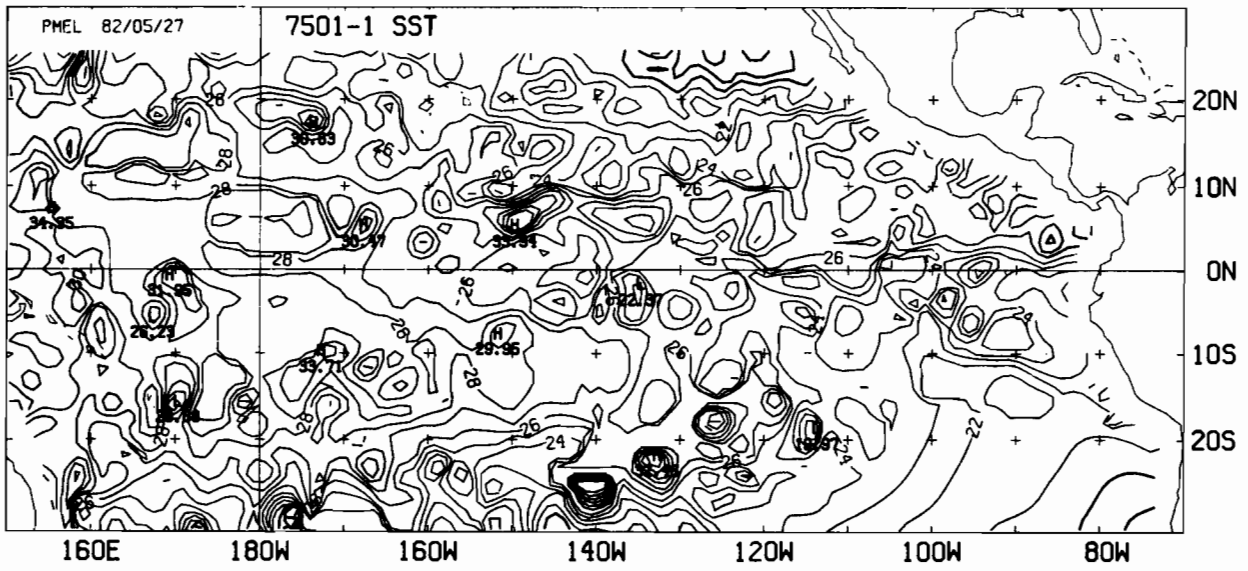

Fig. 2.2

Fig. 2.3

in changing variances and patterns of data sets? We shall examine and answer most of these questions as a matter of course in the following sections. It will turn out that an objectively analyzed data set can be *significantly* affected in any one of its three main attributes (location, spread, pattern) by data density and by retaining or dropping this or that feature from an objective analysis scheme.

One main conclusion we shall reach is that: climate diagnoses and climate forecasts, based on two differently "objectively" analyzed data fields, can possibly be affected by significant differences in the locations, spreads, and patterns of the two resultant data sets.

3. Rule N and Rule Q Applied to the Liu Set

To gain an initial impression of the relative signal and noise content of the Liu data set, we applied* Rule N and Rule Q to the Liu data set on a subset of 21 equally spaced points over a rectangular equatorial region from 10°N to 10°S and 80°W to 200°W. We used 72 monthly averages over the period January 1975 to December 1980. Hence, in the terminology of the two Rules, $p = 21$ and $n = 72$.

Fig. 3.1 shows the result of the N Rule applied to Liu's data set. This suggests that the first two (and perhaps first three) eigenvectors should be retained as the dominant-variance signal-bearing part of the data set, on the basis that (via Rule N) they are distinguished from eigenvectors produced by spatially and temporally homogeneous noise. On the other hand, Rule Q seeks out non random time behavior of the principal components rather than

---

* Preisendorfer, et al. (1981) (p. 99 for Rule N, p. 127 for Rule Q).

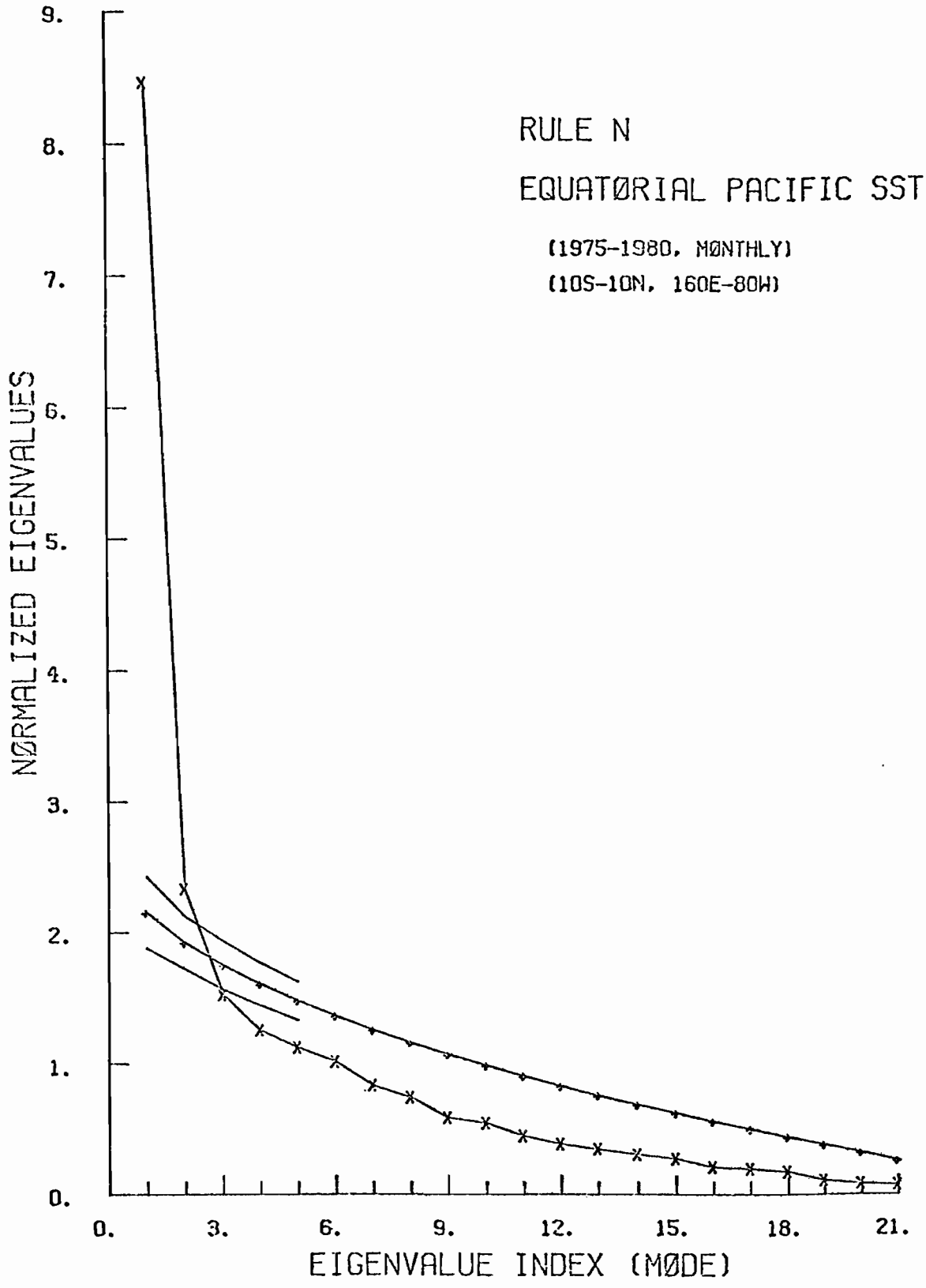
RULE N
EQUATØRIAL PACIFIC SST
(1975-1980, MØNTHLY)
(10S-10N, 160E-80W)
NØRMALIZED EIGENVALUES
EIGENVALUE INDEX (MØDE)
0.
1.
2.
3.
4.
5.
6.
7.
8.
9.
0.
3.
6.
9.
12.
15.
18.
21.

Fig. 3.1

sheer variance domination of the components. Rule Q in Fig. 3.2 says that we should retain the first four eigenvectors as possible carriers of non random temporal behavior. The agreement between the two Rules, considering the diverse attributes of the data set they examine, is remarkably close in the sense that we would, on the basis of either rule, with confidence 95%, decide that the first three eigenmodes (say) are statistically significant. The first three modes are shown in Fig. 3.3. The first mode contains 40% of the SST variance and represents a nearly spatially uniform rising and falling, in time, of the SST over the 20° latitude band surrounding the equator, all the way from 80°W to 200°W. The intuitive reason for Rule Q selecting these first three modes is evident in the non random behavior of the principal component plots over the six-year interval shown below the plot of each eigenvector. Rule Q evidently detected the onset of weak El Niño type behavior on 1976.

In order to place the preceding observations in perspective, we obtained (via Liu) a copy of Weare's SST data set* and excised a portion that is nearly spatially coincident with the Liu set. This time we used p = 30 points and once again the time period was for n = 72 months, over the period 1949-1954. Fig. 3.4 shows Rule N deciding that the first three eigenvalues are statistically significant, while Fig. 3.5 indicates that Rule Q corroborates this decision. Fig. 3.6 plots the first 3 eigenmodes of Weare's data set. The conclusion is that, over the two separate six year intervals on this essentially common equatorial domain, the signal to noise partitions of the data sets by Rules N and Q are much the same. It is interesting to note also that each of these six year intervals contained a weak El Niño (1951, 1976), as may be seen from Fig. 3.3 and Fig. 3.6.

---

* Weare, et al. (1976).

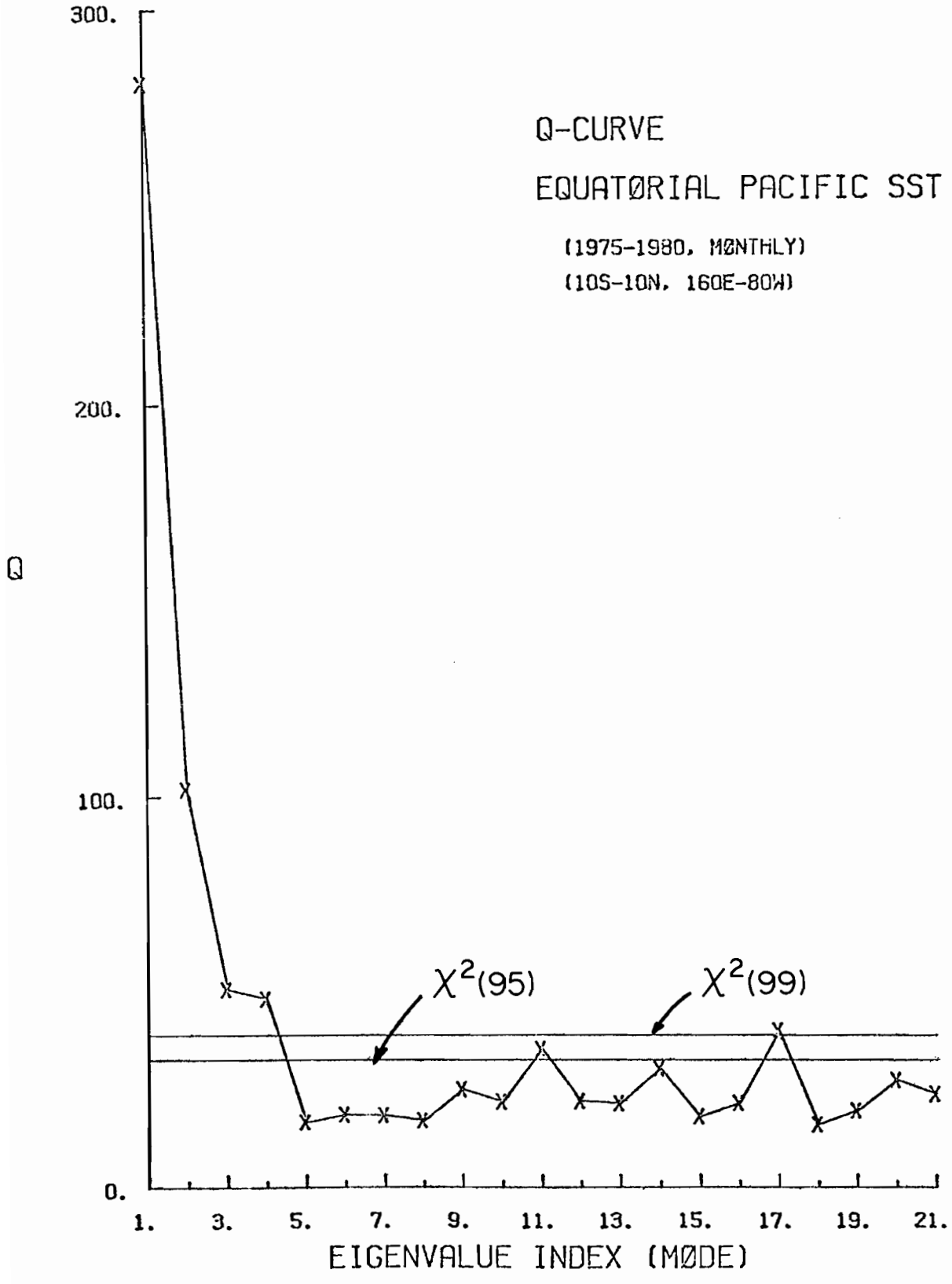
Q-CURVE
EQUATØRIAL PACIFIC SST
(1975-1980, MØNTHLY)
(10S-10N, 160E-80W)
300.
200.
100.
0.
Q
χ^2(95)
χ^2(99)
1. 3. 5. 7. 9. 11. 13. 15. 17. 19. 21.
EIGENVALUE INDEX (MØDE)

Fig. 3.2

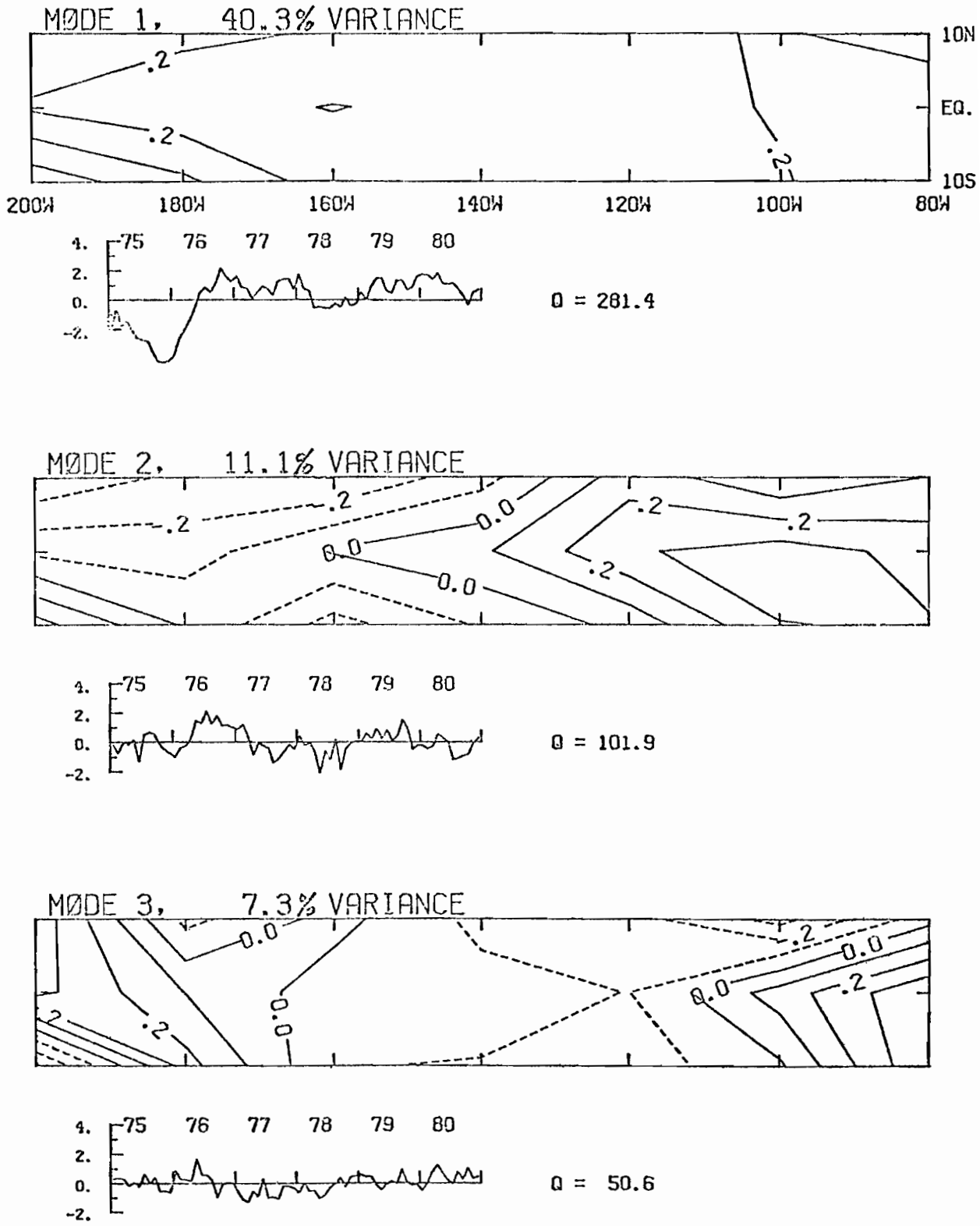
MØDE 1, 40.3% VARIANCE
10N
EQ.
10S
200W
180W
160W
140W
120W
100W
80W
.2
.2
.2
75 76 77 78 79 80
4.
2.
0.
-2.
Q = 281.4
MØDE 2, 11.1% VARIANCE
.2
.2
.2
.2
.2
0.0
0.0
0.0
75 76 77 78 79 80
4.
2.
0.
-2.
Q = 101.9
MØDE 3, 7.3% VARIANCE
0.0
0.0
0.0
.2
.2
.2
.2
75 76 77 78 79 80
4.
2.
0.
-2.
Q = 50.6

Fig. 3.3

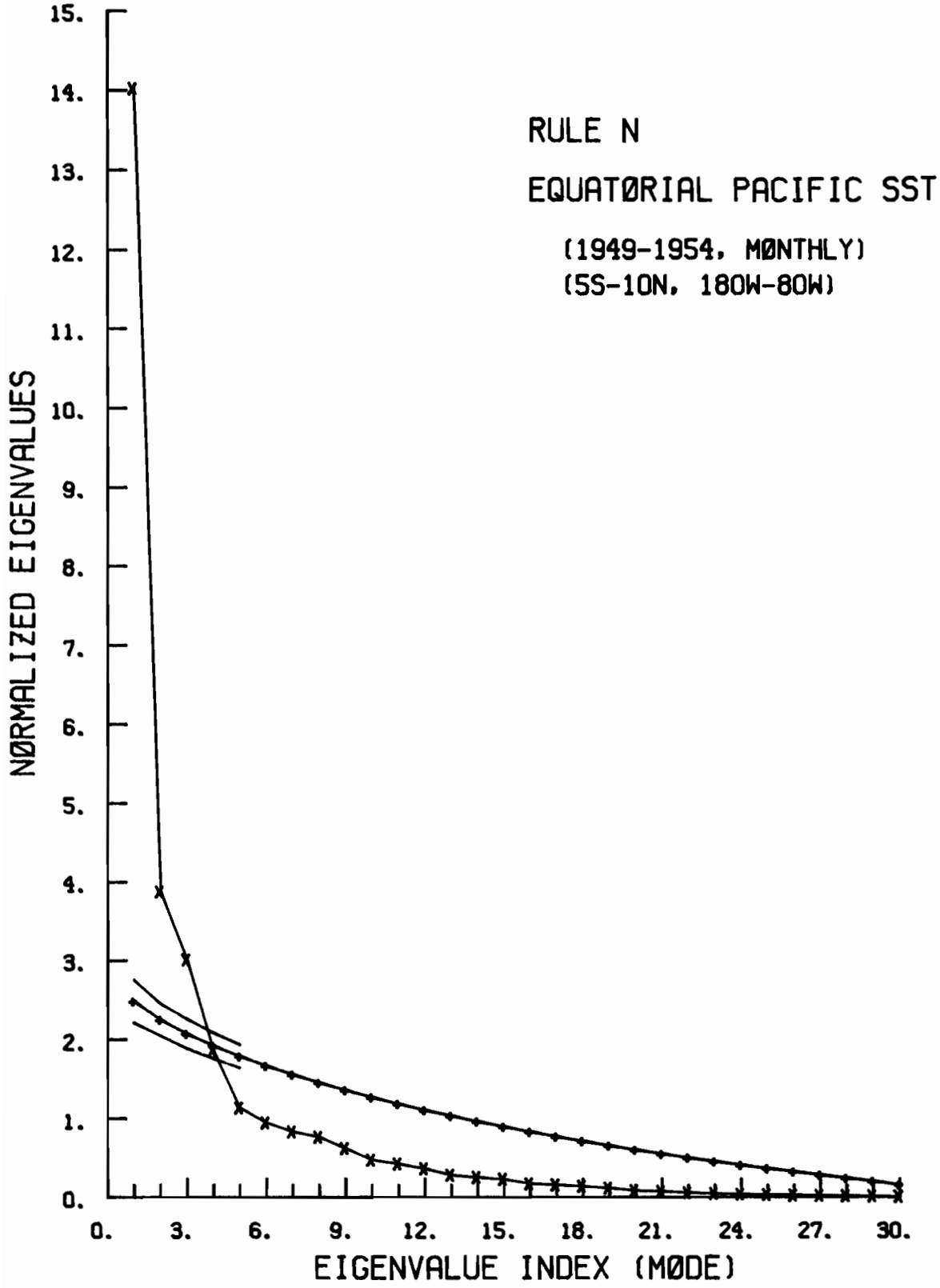
RULE N
EQUATØRIAL PACIFIC SST
(1949-1954, MØNTHLY)
(5S-10N, 180W-80W)
NØRMALIZED EIGENVALUES
EIGENVALUE INDEX (MØDE)
0.
1.
2.
3.
4.
5.
6.
7.
8.
9.
10.
11.
12.
13.
14.
15.
0.
3.
6.
9.
12.
15.
18.
21.
24.
27.
30.

Fig. 3.4

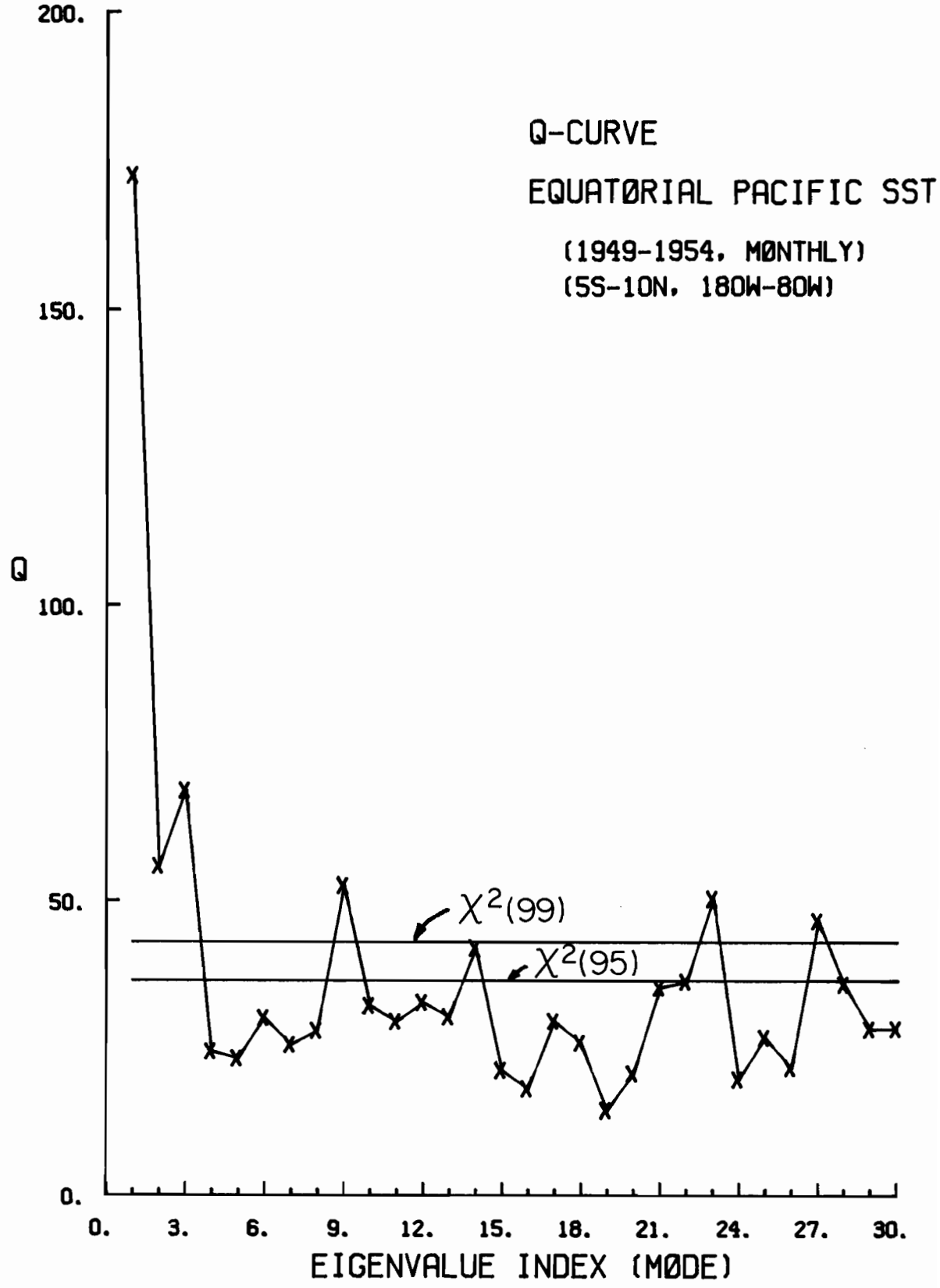
Q-CURVE
EQUATØRIAL PACIFIC SST
(1949-1954, MØNTHLY)
(5S-10N, 180W-80W)
Q
200.
150.
100.
50.
0.
$X^2(99)$
$X^2(95)$
0.
3.
6.
9.
12.
15.
18.
21.
24.
27.
30.
EIGENVALUE INDEX (MØDE)

Fig. 3.5

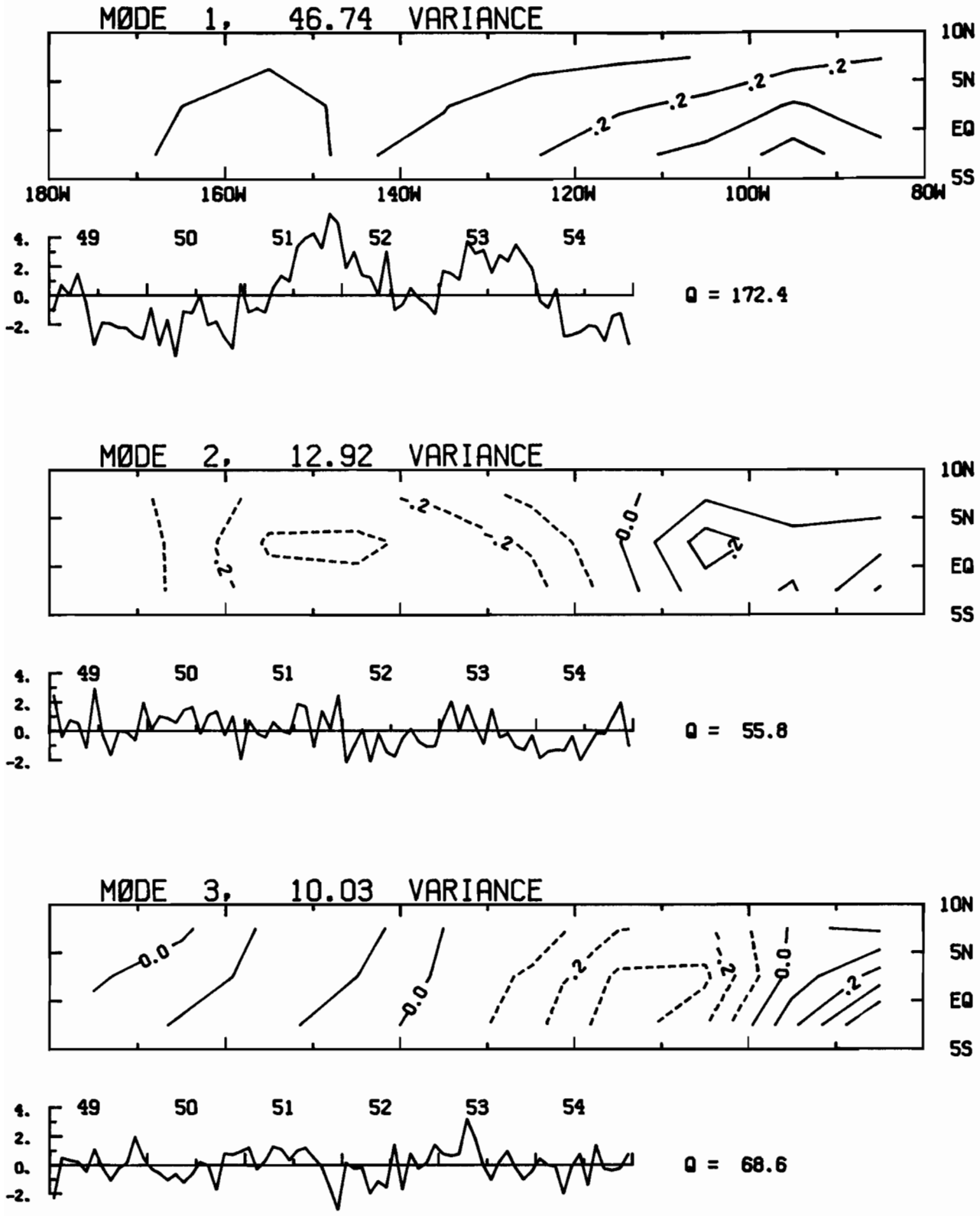
MØDE 1, 46.74 VARIANCE
10N
5N
EQ
5S
180W
160W
140W
120W
100W
80W
.2
.2
.2
.2
4.
2.
0.
-2.
49
50
51
52
53
54
Q = 172.4
MØDE 2, 12.92 VARIANCE
10N
5N
EQ
5S
.2
.2
.2
0.0
.2
4.
2.
0.
-2.
49
50
51
52
53
54
Q = 55.8
MØDE 3, 10.03 VARIANCE
10N
5N
EQ
5S
0.0
0.0
.2
.2
0.0
.2
4.
2.
0.
-2.
49
50
51
52
53
54
Q = 68.6

Fig. 3.6

4. Tercile Tests Applied to the Liu, Modified L-O, and Original L-O Sets

The tercile tests, as described in DIT(IV), were illustrated as a matter of course in that study by means of the present three data sets. It is of interest to collect those illustrations here with the full descriptions of the objective analysis schemes that produced them.

In Fig. 4.1 we have the 99 point region of the Pacific over which the intercomparisons were made. In particular we isolated four 24-point sub-regions according to the amounts of data density and SST-gradient over them. Thus, region 1 is a high density, large gradient region off the coast of Mexico, while region 2 around the Hawaiian island chain is of high data density and small SST gradient. Equatorial regions 3, 4 have moderate to low data density and both have small SST gradient.

The results of the tercile tests applied to the data sets over these four regions are summarized in Figs. 4.2, 4.3, 4.4, which illustrate respectively the location, scale, and pattern tests. The tests are applied to both the Liu vs. modified L-O pair and to the Liu vs. original L-O pair of maps.

In Fig. 4.2 we have the results of the location tests. The four circular dots represent the u,v, scores of Liu vs. modified Lev-Ort in regions 1, 2, 3, 4. The dots cluster in the greatest-fit corner of the diagram, indicating nearly perfect match of the average values of the two maps at each region. The Liu vs. original Lev-Ort pair is also very close in location at all but region 2. Nevertheless, all points in the diagram are on the w = 0 line and to the right of both the 5% m line and the 5% u line, indicating significantly great fits. If the patterns were simply drawn at random, then they would hover around the random fit point. This is the case in Fig. 4.3 for the relative scale in Liu vs. original Lev-Ort, indicating that removal of all of Liu's special operations produces two randomly disparate variance

FOUR REGIONS (5° x 10°) FOR DATA INTERCOMPARISON (24 POINTS EACH)

1 = HIGH DATA DENSITY, LARGE SST GRADIENT
2 = HIGH DATA DENSITY, SMALL SST GRADIENT
3 = MODERATE DATA DENSITY, SMALL SST GRADIENT
4 = LOW DATA DENSITY, SMALL SST GRADIENT

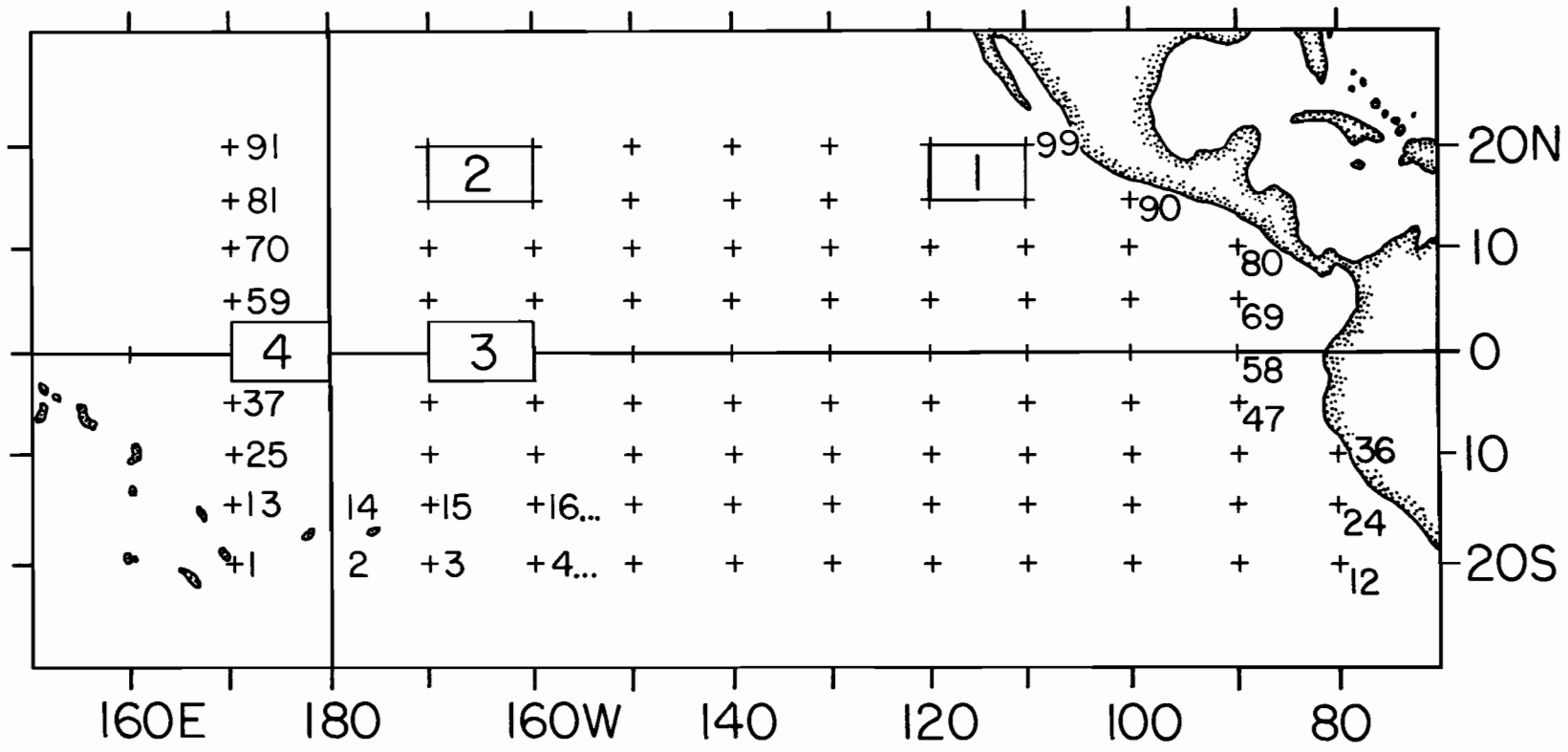

99-POINT DATA SET FOR PREDICTABILITY

Fig. 4.1

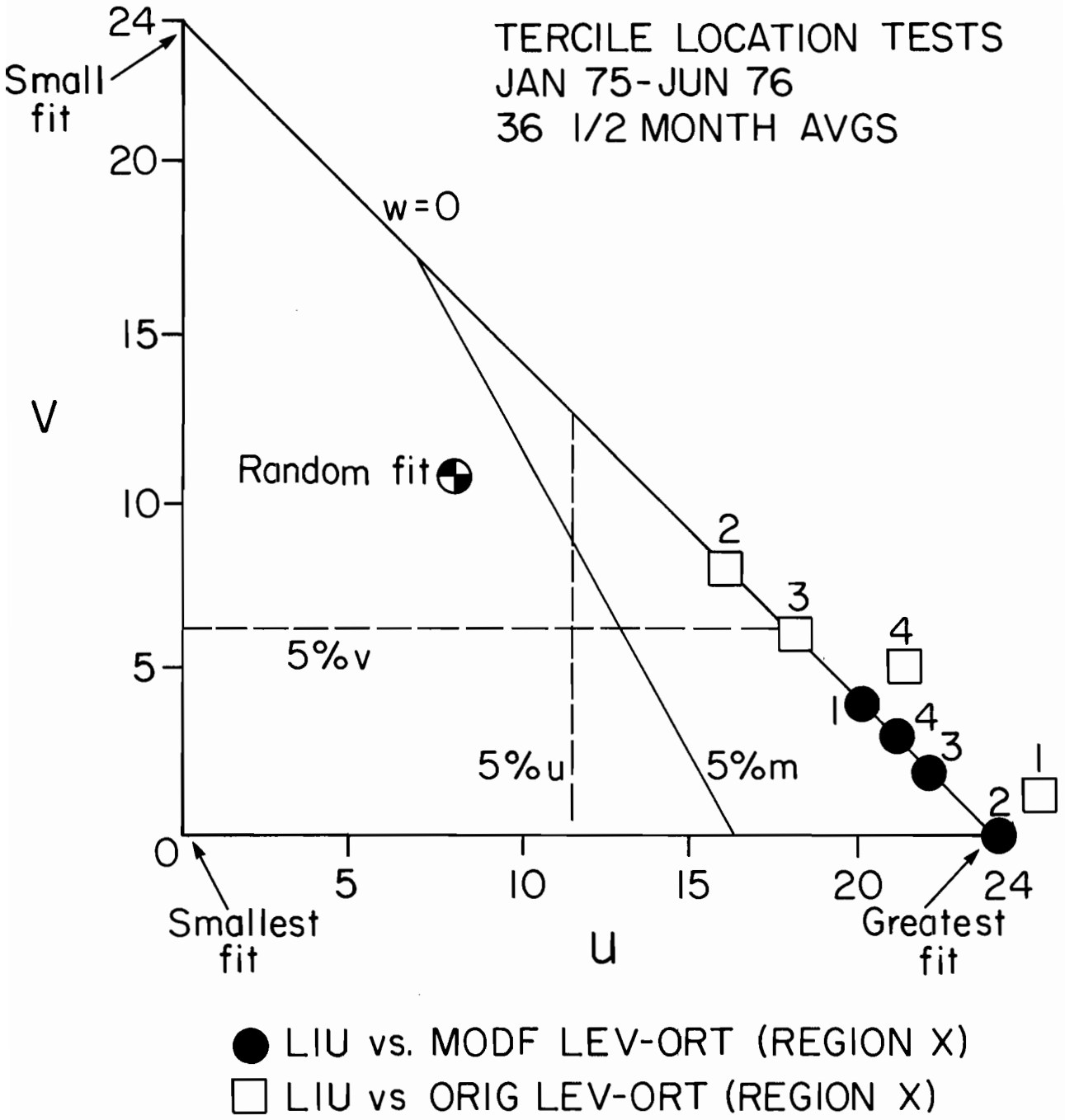
TERCILE LOCATION TESTS
JAN 75-JUN 76
36 1/2 MONTH AVGS
Small fit
w=0
Random fit
5%v
5%u
5%m
V
u
0
5
10
15
20
24
Smallest fit
Greatest fit
LIU vs. MODF LEV-ORT (REGION X)
LIU vs ORIG LEV-ORT (REGION X)

Fig. 4.2

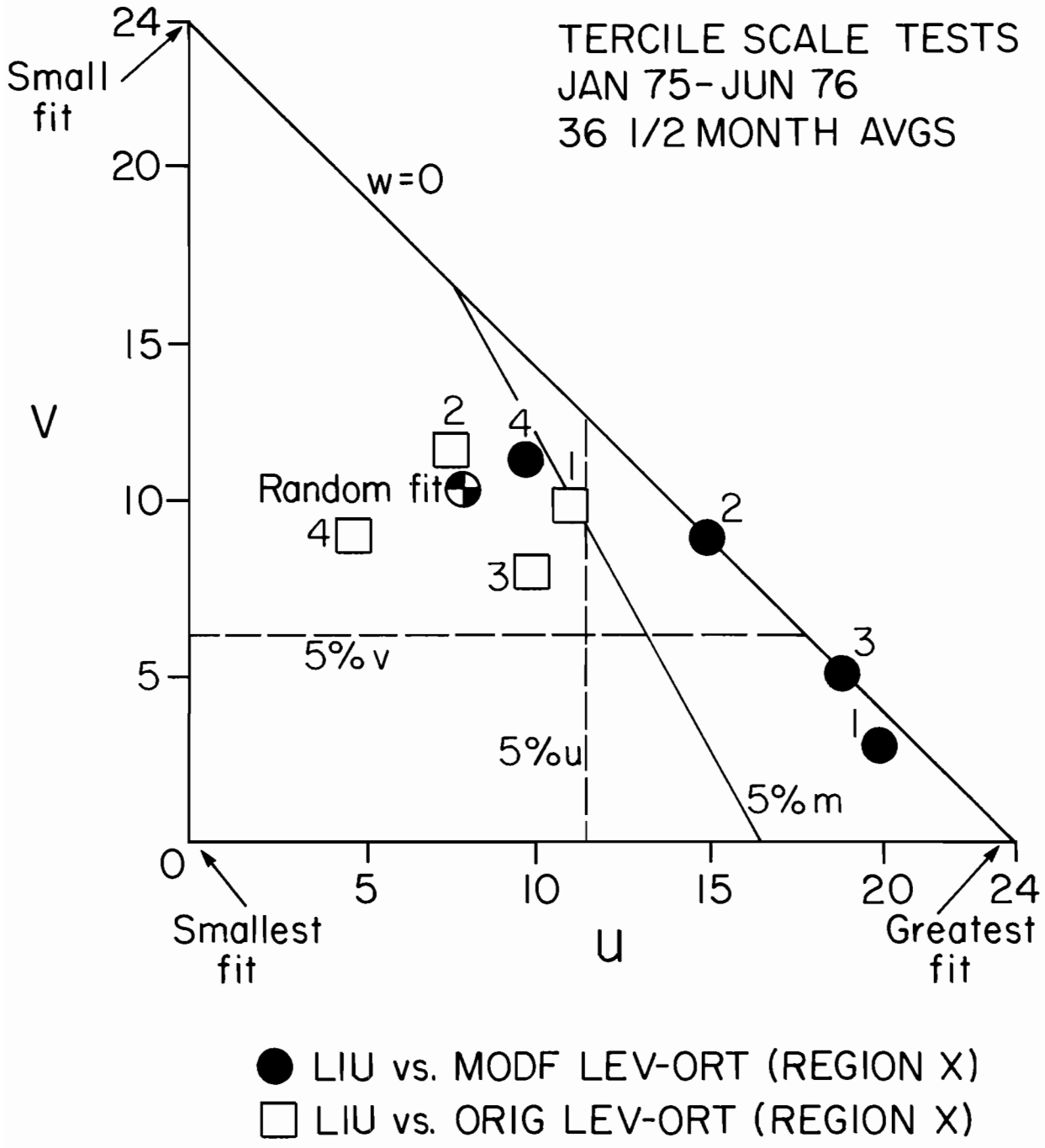
TERCILE SCALE TESTS
JAN 75-JUN 76
36 1/2 MONTH AVGS
Small fit
w=0
Random fit
5% v
5% u
5% m
V
u
0
5
10
15
20
24
Smallest fit
Greatest fit
LIU vs. MODF LEV-ORT (REGION X)
LIU vs. ORIG LEV-ORT (REGION X)

Fig. 4.3

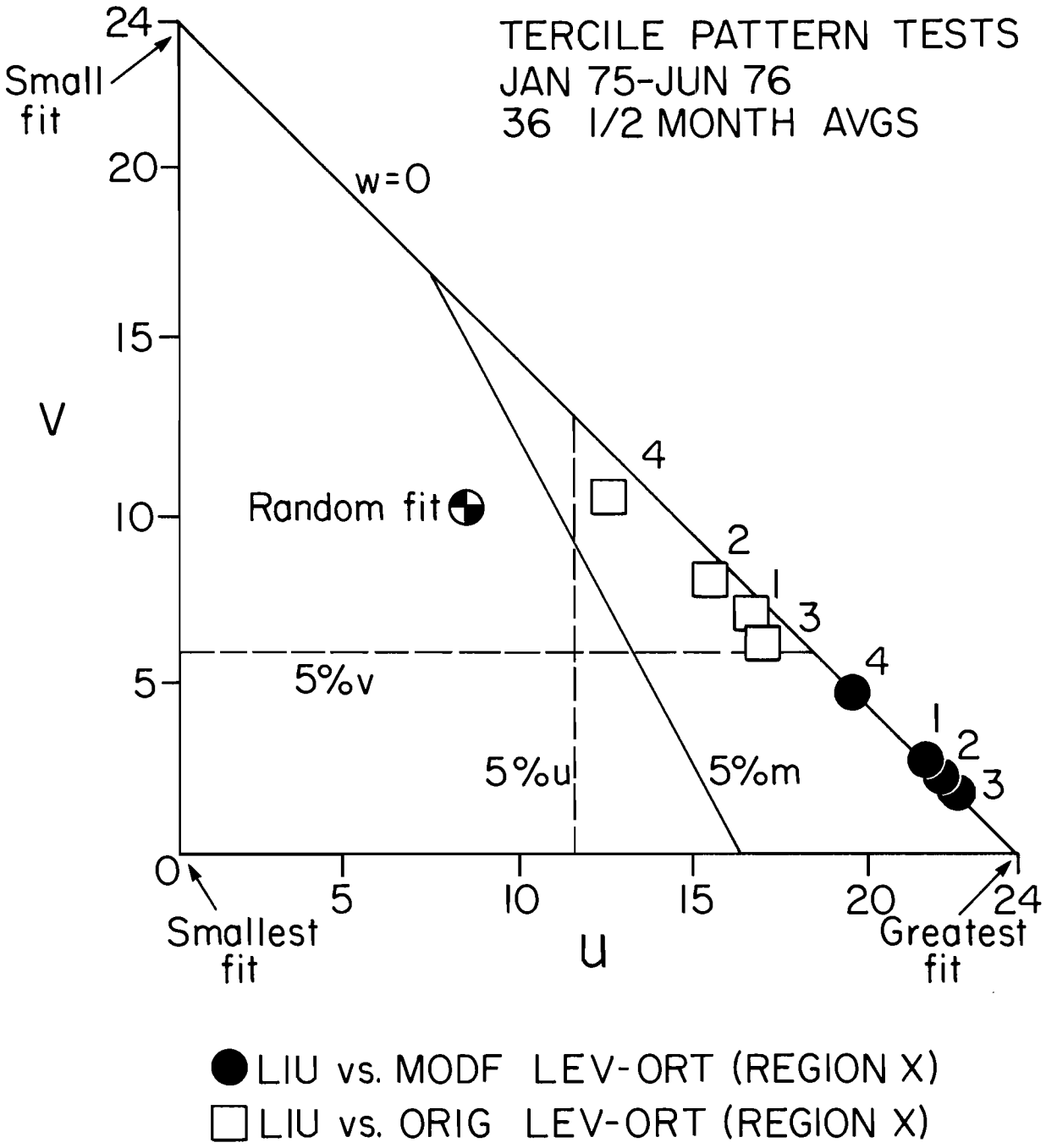
TERCILE PATTERN TESTS
JAN 75-JUN 76
36 1/2 MONTH AVGS
Small fit
w=0
Random fit
5%v
5%u
5%m
V
U
0
5
10
15
20
24
Smallest fit
Greatest fit
LIU vs. MODF LEV-ORT (REGION X)
LIU vs. ORIG LEV-ORT (REGION X)

Fig. 4.4

distributions for Liu and original Lev-Ort over each of the four regions, regardless of data density and SST gradients. In Fig. 4.4 we have corroboration once again of our earlier conclusions in DIT(IV): Liu and modified Lev-Ort are significantly close as regards spatial pattern. The pattern fit between Liu and original Lev-Ort is less close but still significantly close as regards the u and m measures (but not the v-measure).

In sum, we see that removing the data-weight and SST dependent features of Liu's scheme produces no significant change in location, scale, and spatial pattern in high data density and large SST gradient regions. Reducing Liu's scheme to the original Levitus-Oort procedure produces significantly different scale (variance) properties in all data density and SST gradient regions.

We examine next the temporal variations of the spatial patterns of the Liu vs. modified L-O pair of data sets. First of all, we compare their patterns over the entire data domain using the 99-point subset defined in Fig. 4.1. The intercomparison is summarized in Table 4.1.

If the match between the two data maps were that of two *randomly* chosen patterns then the u,v, and w scores in Table 4.1 would average out to be respectively 33, 44, and 22. If the patterns are closer than chance would allow, then the average of u will be higher than 33 and the averages of v,w will then be lower than 44, 22 respectively. The 5% significance level for u is 41, while those for v,w are respectively 36, 15. A perfect fit between two maps would have u = 99, v = w = 0. As it stands in Table 4.1, the close fit between the two maps is extraordinarily* significant, indicating that there is

---

* The Stochaster's behavior will cast this in perspective. The Stochaster's standard deviations for u,v,w are $\sigma_u = 4.69$, $\sigma_v = 4.94$, $\sigma_w = 4.14$. His u,v,w scores are distributed approximately normally about the average values $\bar{u} = 33$, $\bar{v} = 44$, $\bar{w} = 22$. Under these conditions, a positive deviation of u,v,w from $\bar{u},\bar{v},\bar{w}$ by 1.64 σ's is on the threshold of the 5% significance level. The average u,v,w scores at the base of Table 4.1 deviate from 33, 44, 22, respectively, 11.15, 6.23, and 5.17 times the Stochaster sigmas σ_u, σ_v, σ_w. These deviations are large compared to 1.64.

Table 4.1

Tercile Pattern Test Scores of Liu vs. Modified Lev-Ort over 99-Point Region of Fig. 4.1 for ½ month periods January 1975 - June 1976.

	Period	u	v	w
1	1/1/75	82	17	0
2	1/2/75	86	13	0
3	2/1/75	83	16	0
4	2/2/75	82	17	0
5	3/1/75	87	9	3
6	3/2/75	89	10	0
7	4/1/75	84	15	0
8	4/2/75	84	14	1
9	5/1/75	76	21	2
10	5/2/75	85	12	2
11	6/1/75	87	12	0
12	6/2/75	89	10	0
13	7/1/75	86	13	0
14	7/2/75	87	12	0
15	8/1/75	78	19	2
16	8/2/75	87	11	1
17	9/1/75	89	10	0
18	9/2/75	82	15	2
19	10/1/75	89	10	0
20	10/2/75	88	11	0
21	11/1/75	89	7	3
22	11/2/75	93	6	0
23	12/1/75	88	11	0
24	12/2/75	87	12	0
25	1/1/76	94	5	0
26	1/2/76	91	8	0
27	2/1/76	87	12	0
28	2/2/76	86	13	0
29	3/1/76	86	13	0
30	3/2/76	85	14	0
31	4/1/76	88	11	0
32	4/2/76	89	9	1
33	5/1/76	81	18	0
34	5/2/76	81	18	0
35	6/1/76	73	25	1
36	6/2/76	72	25	2
AVERAGE		85.3	13.2	.6
STD DEV		4.9	4.6	.9

practically no difference between the two patterns. We conclude that, by dropping the SST-dependent and data-weight features in Liu's scheme, we have essentially left undisturbed the pattern of the original Liu data set. This conclusion evidently holds for each of the 36 pairs of maps over the 36 ½ month periods.

We next divide the 99-point domain into three regions, the west, central, and east region, as shown in Fig. 4.5. These regions have respectively 36, 27, and 36 points. The tercile pattern test of DIT(IV) was applied to the Liu vs. modified L-O pair over each of these subregions. A plot of the u score, as a function of time, of Liu vs. modified L-O, over each region, is shown in Fig. 4.6. For example, the curve connecting the numeral "1" is for the west region, and similar notations hold for the other two regions. A perfect fit between the two maps over the western and eastern regions would yield u = 36. As we can see, the fits over these regions are very significant and approximately of the same high quality. The fit between Liu vs mod L-O over the central region is also of about the same level of significance since the perfect score there would be u = 27.

These findings are summarized in a different way in Table 4.2. There we have recorded significance-level tests over each region as a function of time. If the fits in Fig. 4.6 were uniformly good over the three regions at each time period then there would be no + or - marks in Table 4.2. These marks indicate applications of the hypergeometric distribution theory (see, e.g., DIT(IV)) to the three regions using the u-scores of Fig. 4.6. Only when the local regional u score was below the 10% confidence level or above the 90% confidence level (respectively, above the 90% significance level or below the 10% significance level) did we note the fact in Table 4.2 for the period concerned. Thus in periods 1 to 4 inclusive, e.g., the high u-scores were uniformly distributed over the three regions. In period 5 the west region fit

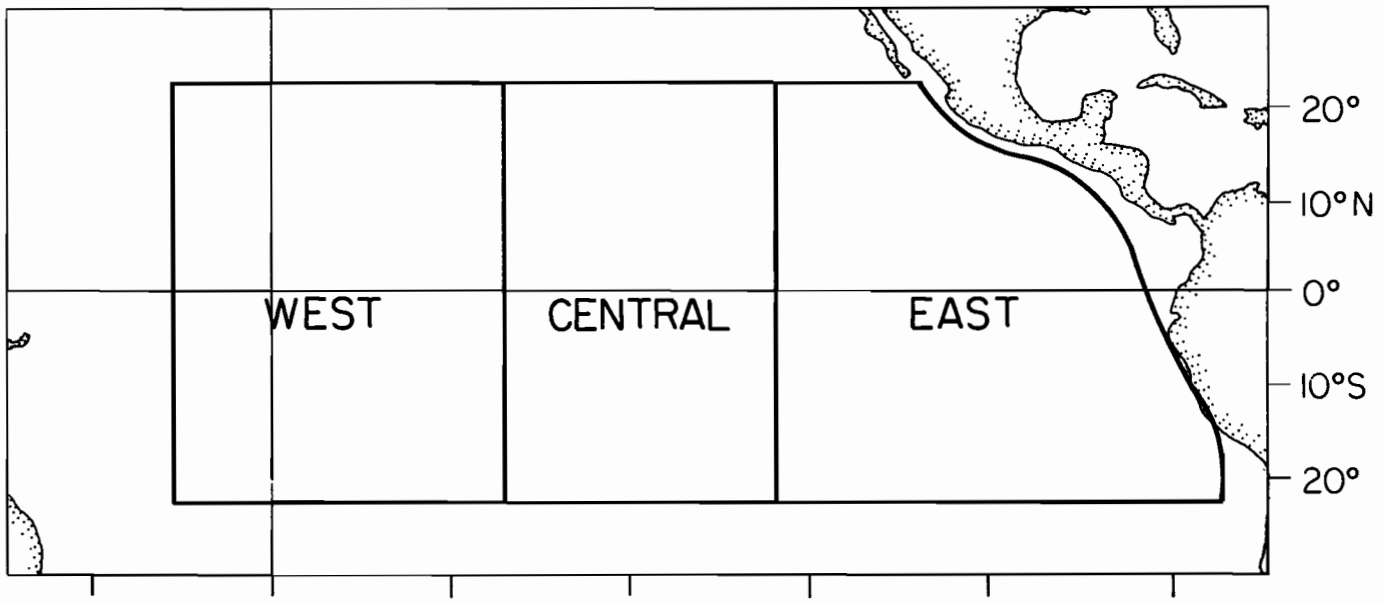

Fig. 4.5

(Fig. 4.6 on p. 26)

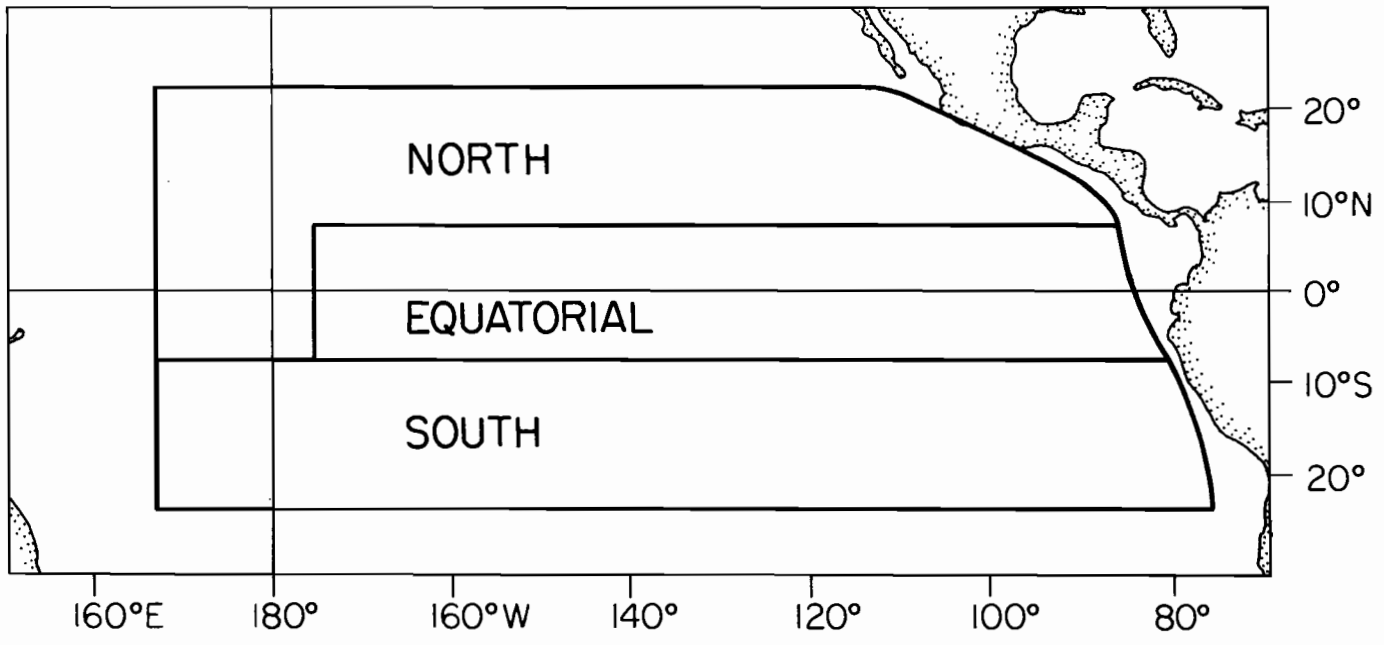

Fig. 4.7

TERCILE TEST FOR LIU vs MODIFIED LEV-ORT IN 36-POINT WEST (=1) AND EAST (=3) AND 27-POINT CENTRAL (=2) JANUARY 1975-JUNE 1976

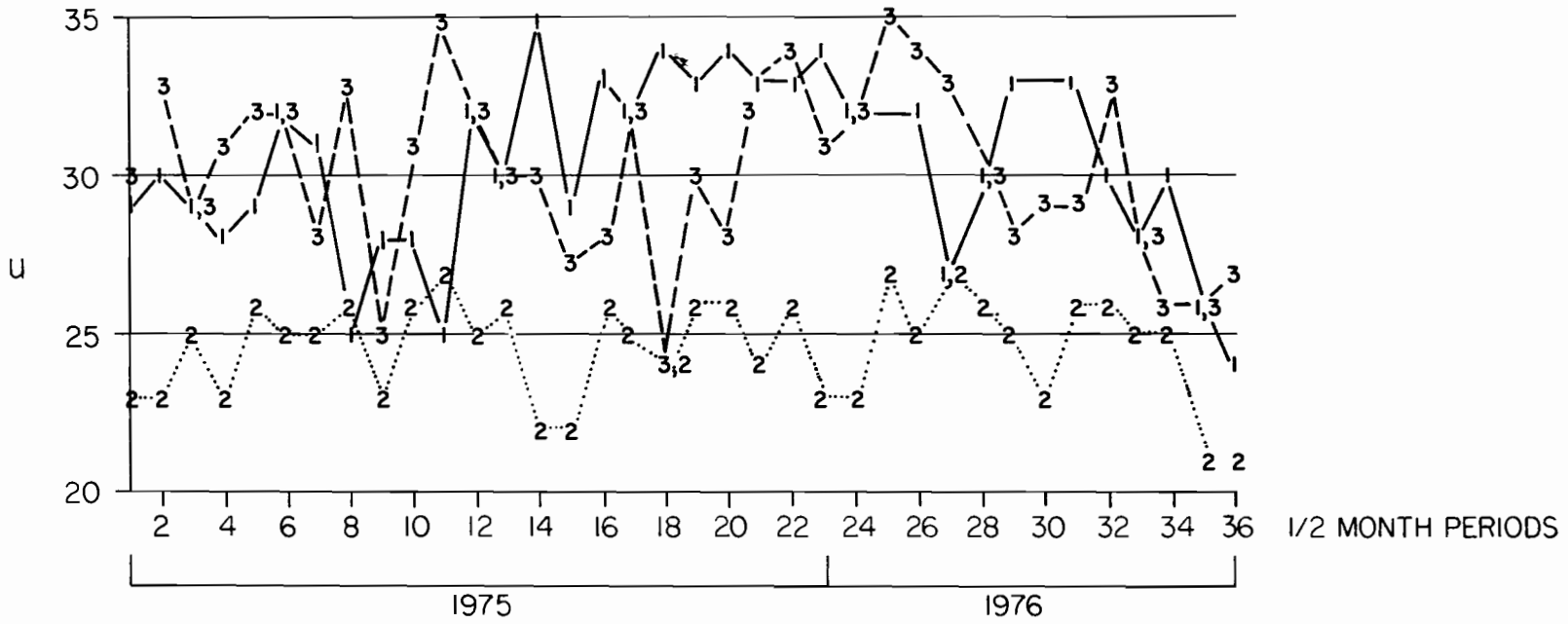

Fig. 4.6

Table 4.2

Tercile Pattern Test Scores of Liu vs. Modified Lev-Ort over West, Central, and East Regions of Fig. 4.5 for ½ Month Periods January 1975 - June 1976.

	Period	West	Cent.	East
1	1/1/75			
2	1/2/75			
3	2/1/75			
4	2/2/75			
5	3/1/75	-		
6	3/2/75			
7	4/1/75			
8	4/2/75	-	+	
9	5/1/75			
10	5/2/75	-	+	
11	6/1/75	-	+	+
12	6/2/75			
13	7/1/75		+	
14	7/2/75	+		
15	8/1/75			
16	8/2/75			-
17	9/1/75			
18	9/2/75	+		-
19	10/1/75			-
20	10/2/75			-
21	11/1/75			
22	11/2/75			
23	12/1/75			
24	12/2/75			
25	1/1/76	-		
26	1/2/76			
27	2/1/76	-	+	
28	2/2/76		+	
29	3/1/76			-
30	3/2/76			
31	4/1/76			-
32	4/2/76	-		
33	5/1/76		+	
34	5/2/76		+	-
35	6/1/76			
36	6/2/76			

+(-) indicates significance of the regional u at the nominal 90(10) percent confidence level.

between the two maps was poorer, being below the 10% confidence level. In period 8, the central region had a better fit, above the 90% confidence level, while the west region's fit fell below the 10% level.

The main point to observe from Table 4.2 is that *the very significantly good fits between Liu vs. modified Lev-Ort seen over the entire Pacific domain in Table 4.1 are distributed fairly uniformly in the east-west extent of the domain.* Very seldom in the Table at any one period are *all three* or *even two* regions deviating significantly from their expected middle-ground-fits (between 10% to 90% confidence).

Finally, we divide the 99-point domain into three regions, the north, equatorial, and south regions, as shown in Fig. 4.7. These regions have, respectively, 36, 27, and 36 points. The Tercile Pattern Test of DIT(IV) was applied to the Liu vs. modified L-O pair over each of these subregions. Table 4.3 shows how the excellent fits of Table 4.1 are partitioned in these new regions. Once again, as in Table 4.2, a scarcity of + or - marks indicates (via the hypergeometric distribution) a uniformly good fit over the whole expanse of the Pacific domain, now partitioned in the north, equatorial, and south subregions. We observe that the fit over the equatorial region is (with only 2 departures from ordinary fits) extremely uniform in time: the two data sets are practically indistinguishable over this subregion, period after period. During this same stretch of periods, the north subregion has 9 departures from ordinary fits, while the southern subregion has 7 departures from ordinary fits. The number of departures (+,-) and the sign changes of each set of departures are compatible with simple chance fluctuations.

In sum, then, the SST patterns of the Liu and modified Levitus-Oort data sets are seen by the Tercile Pattern Test to be significantly close and uniformly alike over the whole extent of the 99-point domain during the 18 month period January 1975 - June 1976.

Table 4.3

Tercile Pattern Test Scores of Liu vs. Modified Lev-Ort over North, Equatorial, and South Regions of Fig. 4.7 for ½ Month Periods January 1975 - June 1976.

	Period	South	Equat.	North
1	1/1/75			
2	1/2/75			+
3	2/1/75			
4	2/2/75		+	
5	3/1/75			
6	3/2/75	+		-
7	4/1/75			
8	4/2/75			
9	5/1/75			+
10	5/2/75			
11	6/1/75			
12	6/2/75			-
13	7/1/75			+
14	7/2/75	-		+
15	8/1/75			
16	8/2/75			
17	9/1/75			
18	9/2/75			+
19	10/1/75			
20	10/2/75			
21	11/1/75	-		
22	11/2/75			
23	12/1/75			
24	12/2/75			-
25	1/1/76	-		
26	1/2/76			
27	2/1/76			-
28	2/2/76			
29	3/1/76			
30	3/2/76	+		
31	4/1/76	+		
32	4/2/76			
33	5/1/76			
34	5/2/76	-		
35	6/1/76			
36	6/2/76		+	

+(-) indicates significance of the regional u at the nominal 90(10) percent confidence level.

5. SITES and SPRED Tests (via APP) Applied to Liu, Modified L-O, and Original L-O Sets

The tests to be applied here are defined in DIT(II). Samples of the graphical outcomes of the tests are displayed in Figs. 5.1 - 5.16. These outcomes in turn produce the decisions recorded in Tables 5.1, 5.2. For example, let us review how we reached the decision in Table 5.1 on intercomparing Liu vs. original L-O over region 1. Here we have applied the SITES test via APP (Auto-Cross Permutation Procedure) to the Liu and original Levitus-Oort sets defined over the 24 point region of Fig. 4.1. In the terminology of the APP in DIT(II), "Liu" was denoted by "D" and "orig L-O" took the place of "M". The number of samples in D and M are n = 36 (½ month averages over the 18 month period January 1975 - June 1976). Hence D and M are each n×p = 36×24 matrices. The resultant DD and MM auto distributions, based on r = 100 realizations, are shown in Fig. 5.1. The cross distributions DM and MD are shown in Fig. 5.2. In practice, each member of these pairs of distributions in each Figure 5.1, 5.2 should be about the same as the other, and indeed they are sensibly so. (We ordinarily would not show these figures for DD *and* MM, and for DM *and* MD, but for once, here they are.)

The practical part of the test resides in Figs. 5.3 and 5.4. Thus in Fig. 5.3, starting from the median of the DM curve, we go vertically up to the DD curve and intersect it at about the 60% ordinate of the DD curve. In Fig. 5.4 the two MM and MD curves are nearly coincident. Starting from the MD curve and rising vertically to the MM curve, we reach the latter at about the 50% ordinate of the MM curve. In principle (on the basis of the close matches in Figures 5.1, 5.2) this result should be the same as the preceding result. Taking the average of these two readings *we find 55% as the confidence level that Liu and original L-O, as far as SITES is concerned, are drawn from*

REGION I

LIU vs ORIGINAL LEV-ORT

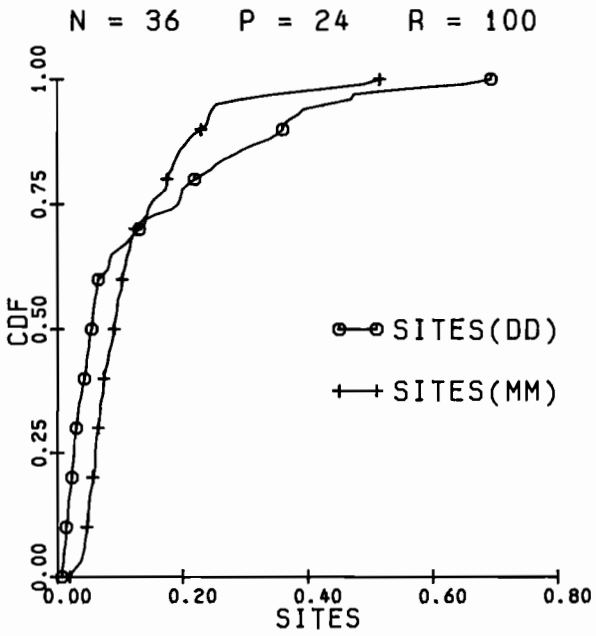

Fig. 5.1

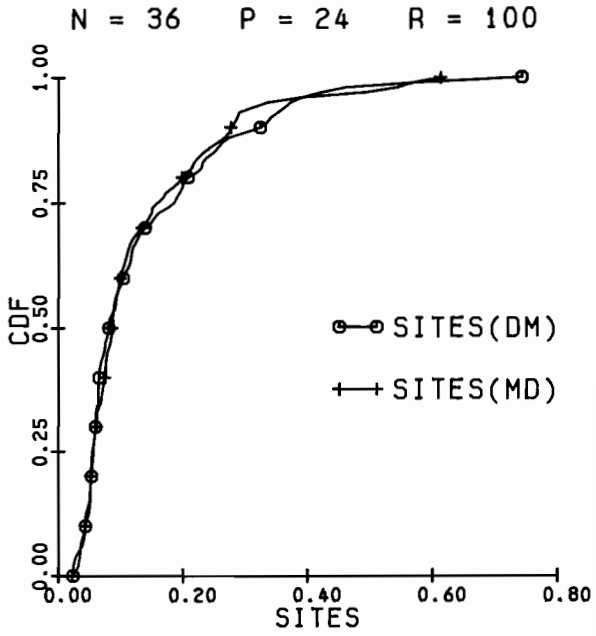

Fig. 5.2

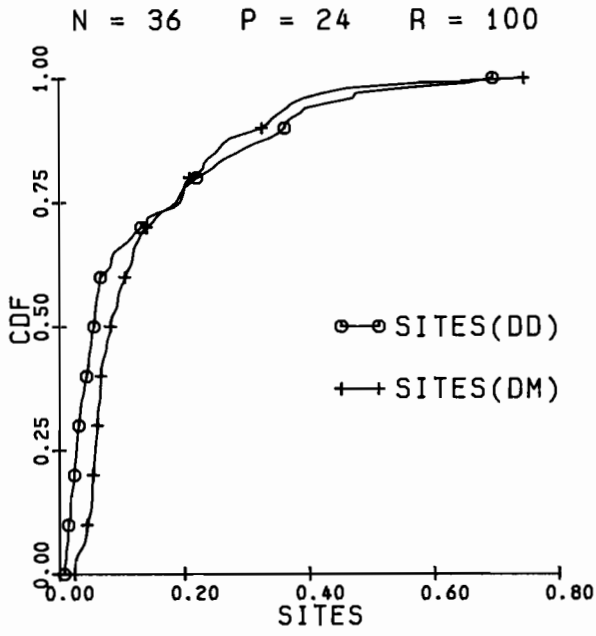

Fig. 5.3

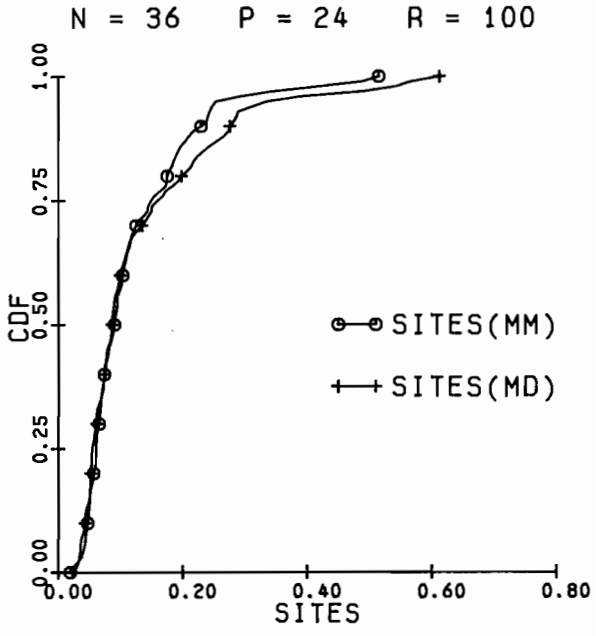

Fig. 5.4

REGION I

LIU vs ORIGINAL LEV-ORT

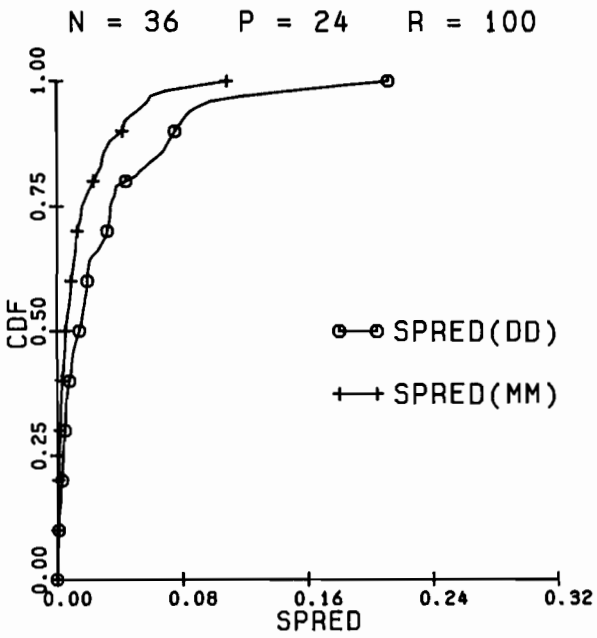

Fig. 5.5

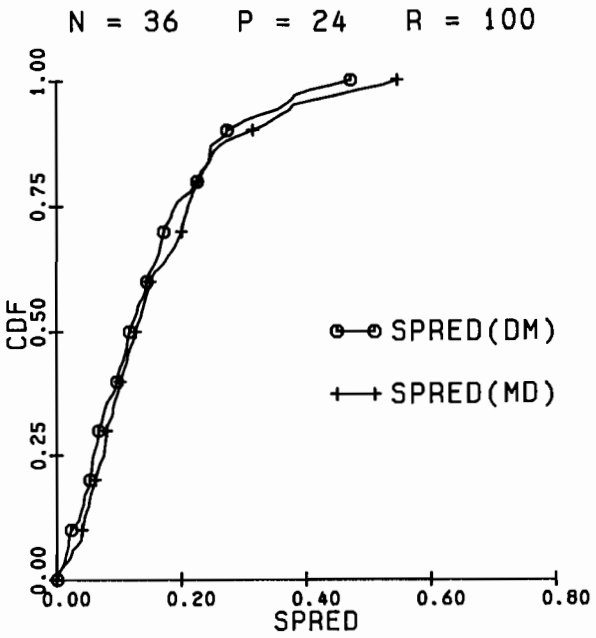

Fig. 5.6

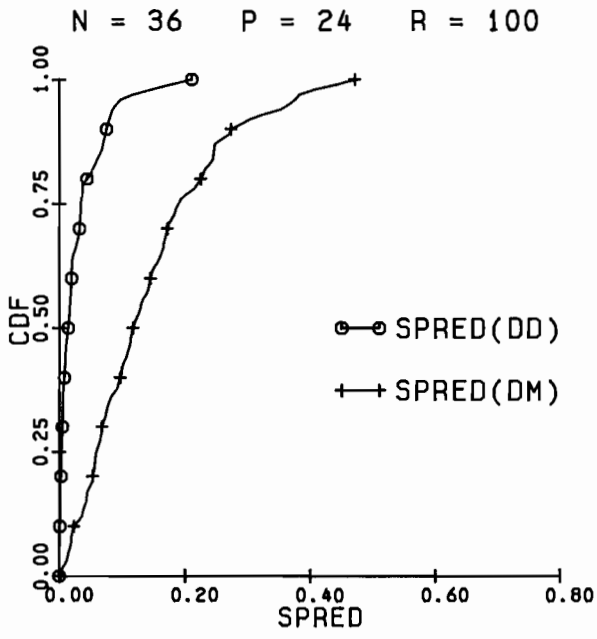

Fig. 5.7

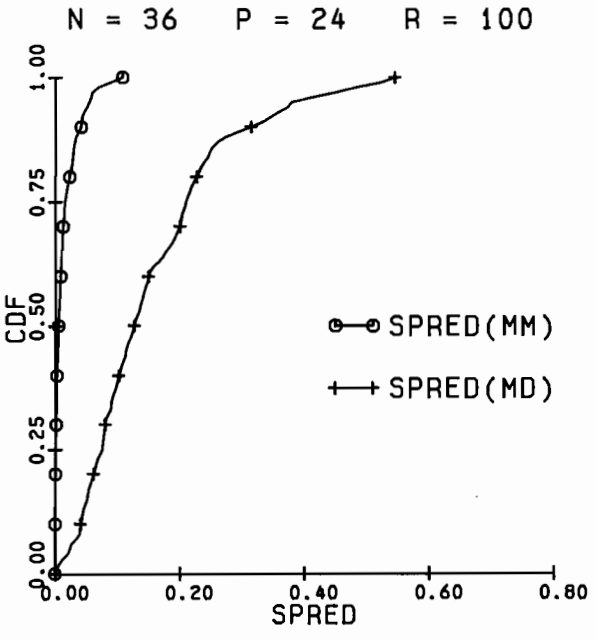

Fig. 5.8

REGION I

LIU vs MODIFIED LEV-ORT

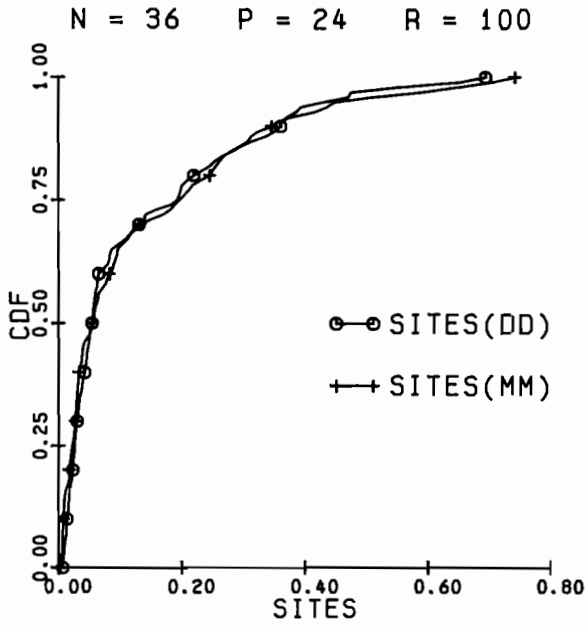

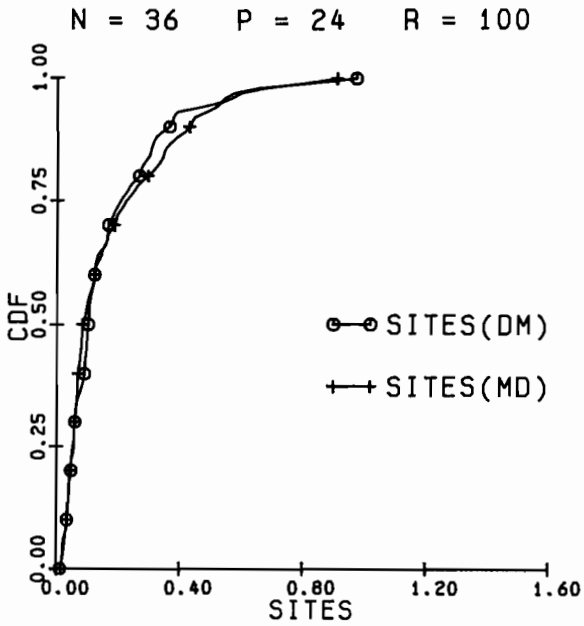

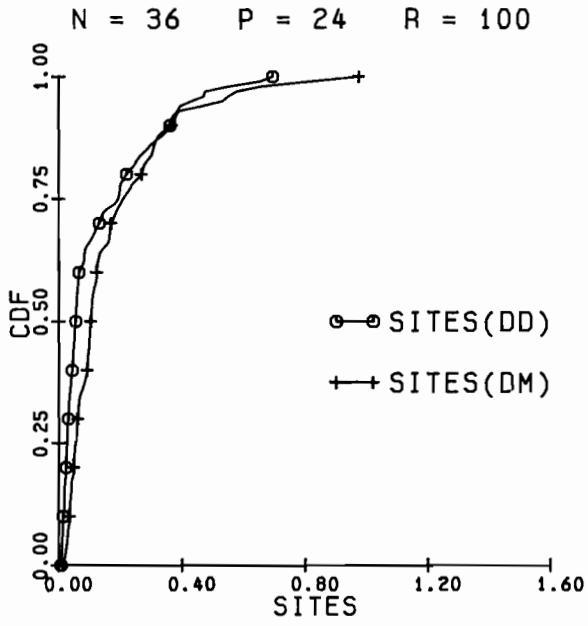

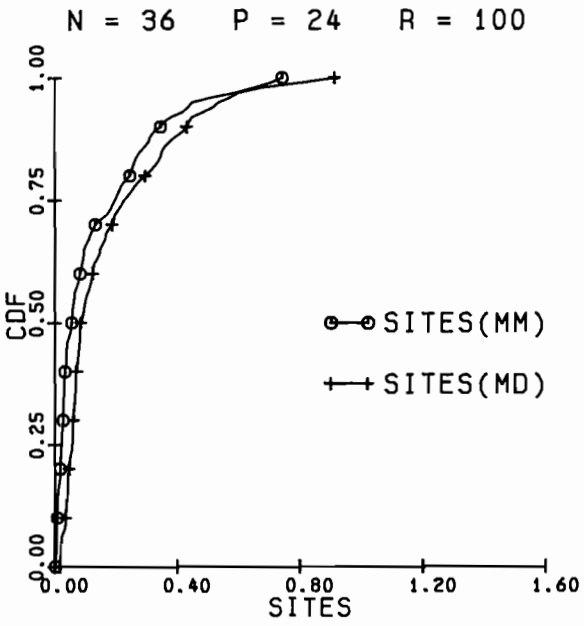

Fig. 5.9 **Fig. 5.10**

Fig. 5.11 **Fig. 5.12**

REGION I

LIU vs MODIFIED LEV-ORT

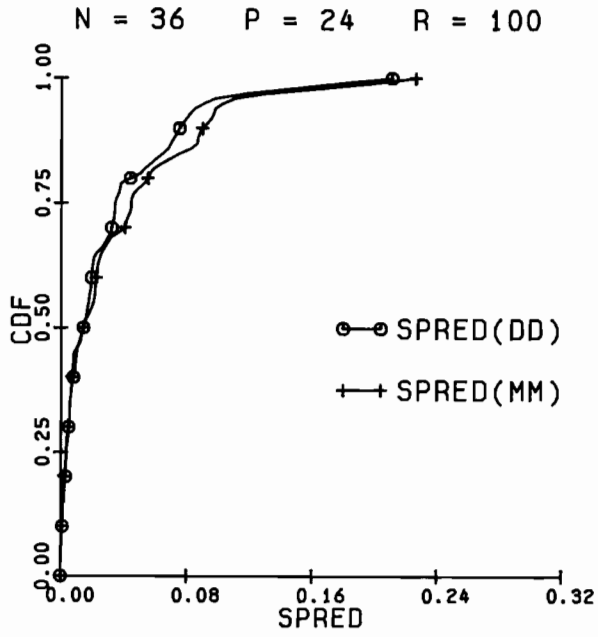

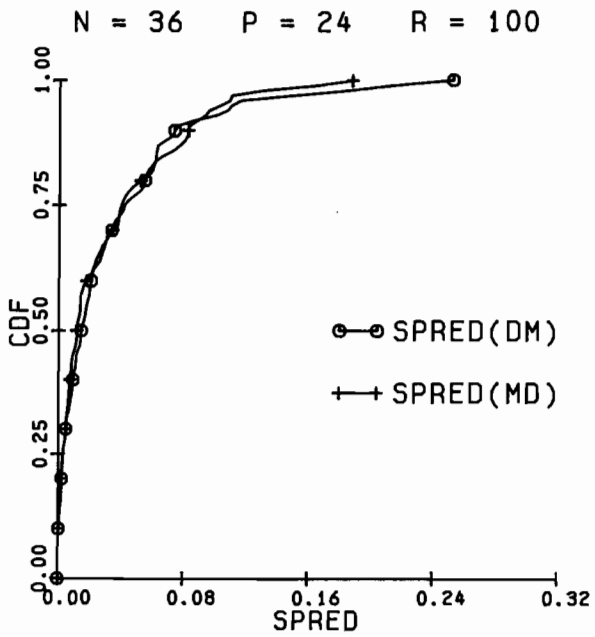

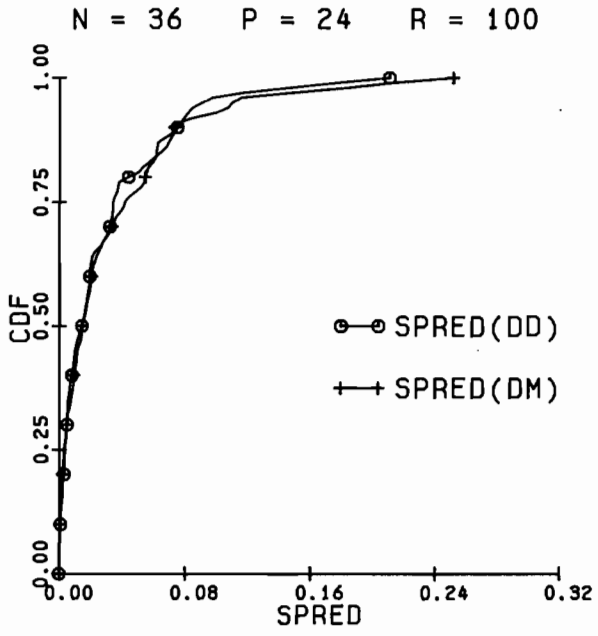

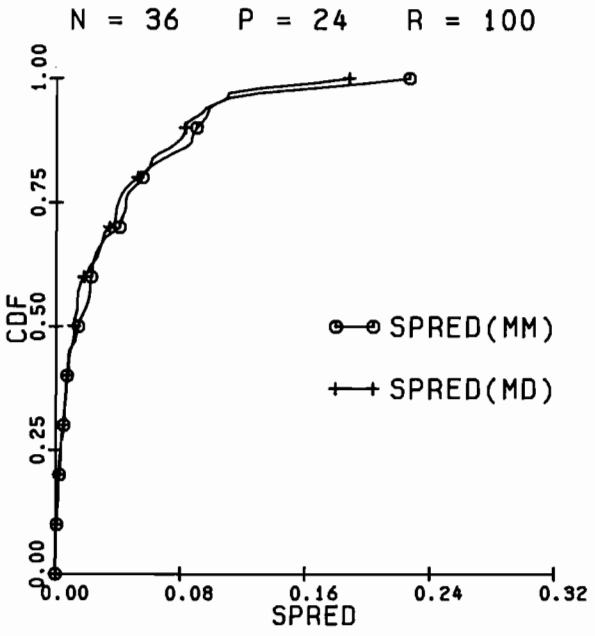

Fig. 5.13 **Fig. 5.14**

Fig. 5.15 **Fig. 5.16**

Table 5.1

SST DATA SET INTERCOMPARISONS
AUTO- AND CROSS-PERMUTATION NOISE PROCEDURE

SITES (DIFFERENCE OF MEANS)

REGION	LIU VS. ORIG L-O		LIU VS. MODF L-O		MODF L-O VS. ORIG L-O	
HIGH DENSITY HIGH GRADIENT 1	SAME	55%	SAME	63%	SAME	72%
HIGH DENSITY HIGH GRADIENT 2	SAME	76	SAME	50	SAME	75
MOD. DENSITY LOW GRADIENT 3	SAME	73	SAME	50	SAME	73
MOD. DENSITY LOW GRADIENT 4	SAME	78	SAME	52	SAME	88

CONFIDENCE LEVEL C

DIFFERENT: CONFIDENCE LEVEL 90% OR MORE

SAME: CONFIDENCE LEVEL 89% OR LESS

Table 5.2

SST DATA SET INTERCOMPARISONS
AUTO- AND CROSS-PERMUTATION NOISE PROCEDURE

SPRED (DIFFERENCE OF VARIANCES)

REGION	LIU VS. ORIG L-O	LIU VS. MODF L-O	MODF L-O VS. ORIG L-O
HIGH DENSITY HIGH GRADIENT 1	DIFF 98%	SAME 50%	DIFF 98%
HIGH DENSITY HIGH GRADIENT 2	DIFF 100	SAME 50	DIFF 99
MOD. DENSITY LOW GRADIENT 3	DIFF 100	SAME 50	DIFF 100
MOD. DENSITY LOW GRADIENT 4	DIFF 100	SAME 55	DIFF 100

CONFIDENCE LEVEL C

DIFFERENT: CONFIDENCE LEVEL 90% OR MORE

SAME: CONFIDENCE LEVEL 89% OR LESS

Table 5.3

REGION 3

SEPARATIONS IN °C

	PSITES	PSPRED
LIU VS ORIG LEV-ORT	0.2125°C	0.5922°C
LIU VS MOD LEV-ORT	0.0364°C	0.00388°C
MOD LEV-ORT VS ORIG LEV-ORT	0.2267°C	0.5883°C

different populations. Observe that, by convention, in Table 5.1, we decide that the populations are *different* if the confidence level is 90% or more, and the *same* if the confidence level is 89% or less. Hence, despite the technical manner of the wording of the above conclusion, we finally decide that the sets are the "same" regarding SITES. The remaining entries of Table 5.1 are found in a completely similar way.

In Figs. 5.5 - 5.8, we go through the same general kind of exercise, but now for SPRED, to find the decision recorded in the region 1, Liu vs. original L-O box of Table 5.2. Here we have applied the SPRED test via APP. Figs. 5.5, 5.6 respectively show the preliminary comparisons of the auto distributions DD, MM and the cross distributions DM, MD. Once again the agreement between these pairs of curves is acceptably good. Turning to Fig. 5.7 we see that, on rising from the median of the DM curve to the DD curve we intersect the latter in the 96% ordinate. In Fig. 5.8 this same exercise, now starting from the median of the MD curve, results in the 100% ordinate on the MM curve. The average of these two ordinates is recorded in the upper left entry of Table 5.2, indicating with confidence 98% that, *as far as the APP-based SPRED test is concerned, Liu and original L-O over region 1 are drawn from different populations.*

In Figs. 5.9 - 5.12 we find that, regarding SITES, with confidence 63%, *Liu vs. modified L-O over region 1 are drawn from different populations*; and in Figs. 5.13 - 5.16, *regarding SPRED, with confidence 50%, Liu vs. modified L-O over region 1 are drawn from different populations.*

It is clear from the forms of these tests that, when the confidence level is 50%, then the populations of SITES or SPRED are apparently the same (because the DM and DD curves, or the MD and MM curves will be essentially coincident). As the confidence level (as determined in these tests) rises

above 50%, the evidence mounts that the populations are distinct regarding the SITES or SPRED properties. As indicated below each Table 5.1, 5.2, we agree to use the word "different" as a descriptor of the sets if the confidence level is 90% or more, otherwise we use the word "same". Hence the single word summaries "diff", "same" in the tables describe at a glance whether the sets are different or the same in these respective properties. *Standing back and surveying the overall results in Tables 5.1, 5.2, we conclude that, as regards location (overall averages) the three data set pairs are the same; and as regards spread (overall variance) Liu vs. modified L-O are the same, but the remaining two pairs (Liu vs. Orig L-O, Modf L-O vs. Orig L-O) are different.* These findings therefore generally agree with the tercile tests of §4.

The pairs of sets in Tables 5.1 and 5.2 are all intercompared with dimensionless statistics. To draw out the physical magnitudes of SITES and SPRED, we define (as in (9.1), (9.2) of DIT(II)):

$$\text{PSITES} \equiv \{ \frac{1}{p} \sum_{x=1}^{p} (d(x) - m(x))^2 \}^{\frac{1}{2}} \tag{5.1}$$

where

$$d(x) = n^{-1} \sum_{t=1}^{n} d(t,x)$$

$$m(x) = n^{-1} \sum_{t=1}^{n} m(t,x)$$

and

$$\text{PSPRED} = |\sigma'_D - \sigma'_M| \tag{5.2}$$

where

$$\sigma'_D = \{ \frac{1}{np} \sum_{t=1}^{n} \sum_{x=1}^{p} (d(t,x) - d(x))^2 \}^{\frac{1}{2}}$$

Thus PSITES and PSPRED are simple measures of average and variance differences for n×p data sets, with the same common dimensions as the uncentered d(t,x), m(t,x) values. By way of illustration, Table 5.3 gives these statistics over region 3. The main thing to notice is that Liu vs. original Lev-Ort has a variance temperature difference on the order of 0.6°C, which is a climatologically important magnitude. Therefore by changing from the original Levitus-Oort scheme to the present Liu scheme of objective analyses we change (actually decrease) the standard deviation of the temperature set by about 0.6°C. This variance change is about the same in all three other regions. The change of the average temperature is on the order of 0.2°C for Liu vs. original Lev-Ort over region 3. Our various tests in this study decide that this is not a significant change (see Table 5.1) on the 10% significance (or 90% confidence) level.

6. Comparison of Eigenstructures of Liu, Modified L-O and Original L-O Sets

A. Rule N

We applied Rule N (cf. §3 above) to the three data sets over regions 1 and 4. The results are shown in Figs. 6.1, 6.2, 6.3. On the basis of all we have seen so far in our intercomparisons of these sets, we could expect the eigenvalue curves of Liu and modified L-O to be fairly close, while that of original L-O to be somewhat different. These expectations are borne out, thereby adding one more angle of view of the attributes of these three sets. For example, in Fig. 6.1, over region 1, the Liu set has one significant eigenvalue of relatively large percentage of the total variance (86.8%). In Fig. 6.2, the first eigenvalue of modified L-O over region 1 is also the only significant one with 90.8% of the total variance. On the other hand, in

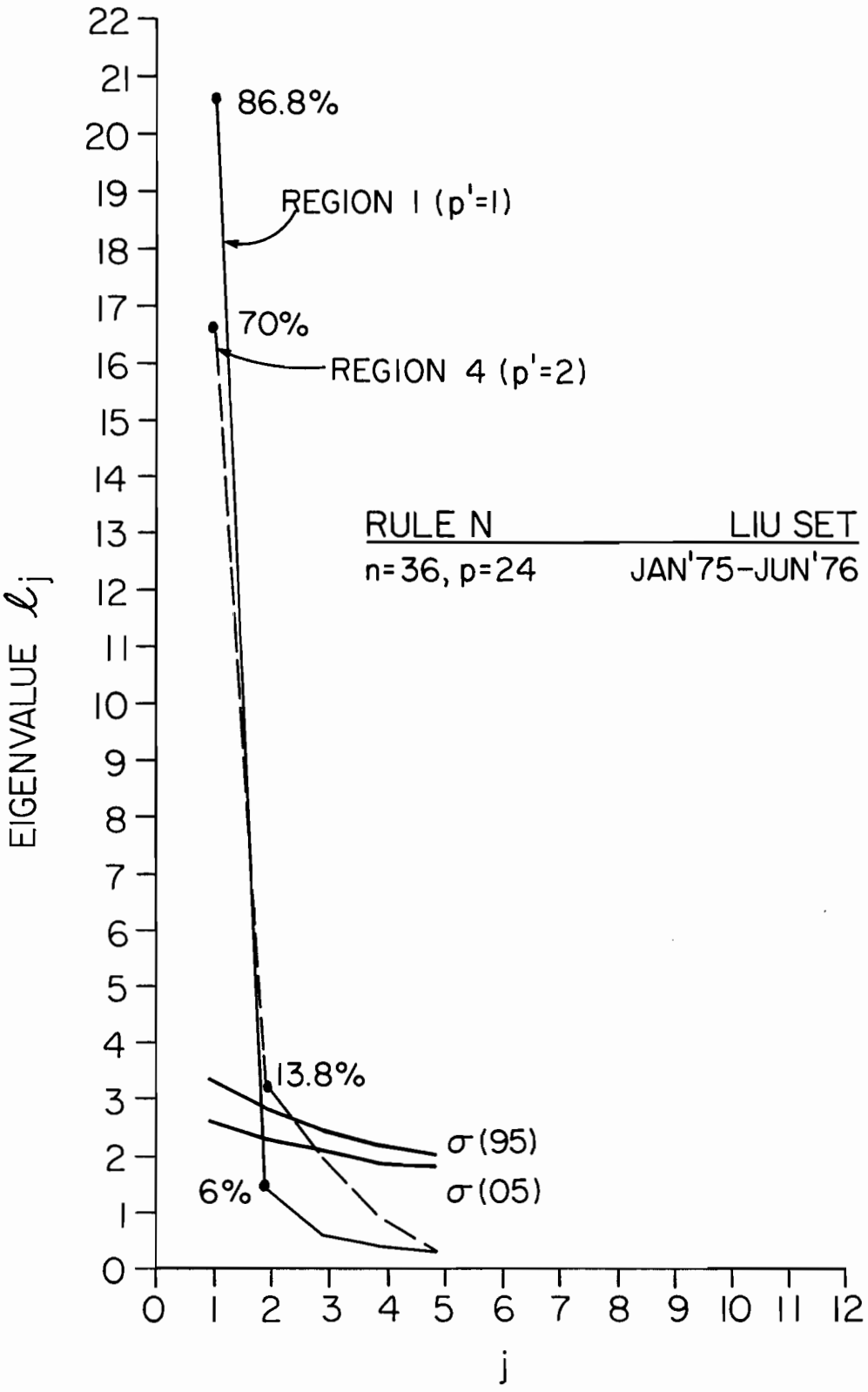
EIGENVALUE ℓ_j
j
86.8%
REGION 1 (p'=1)
70%
REGION 4 (p'=2)
RULE N
LIU SET
n=36, p=24
JAN'75–JUN'76
13.8%
σ(95)
σ(05)
6%
0 1 2 3 4 5 6 7 8 9 10 11 12
0 1 2 3 4 5 6 7 8 9 10 11 12 13 14 15 16 17 18 19 20 21 22

Fig. 6.1

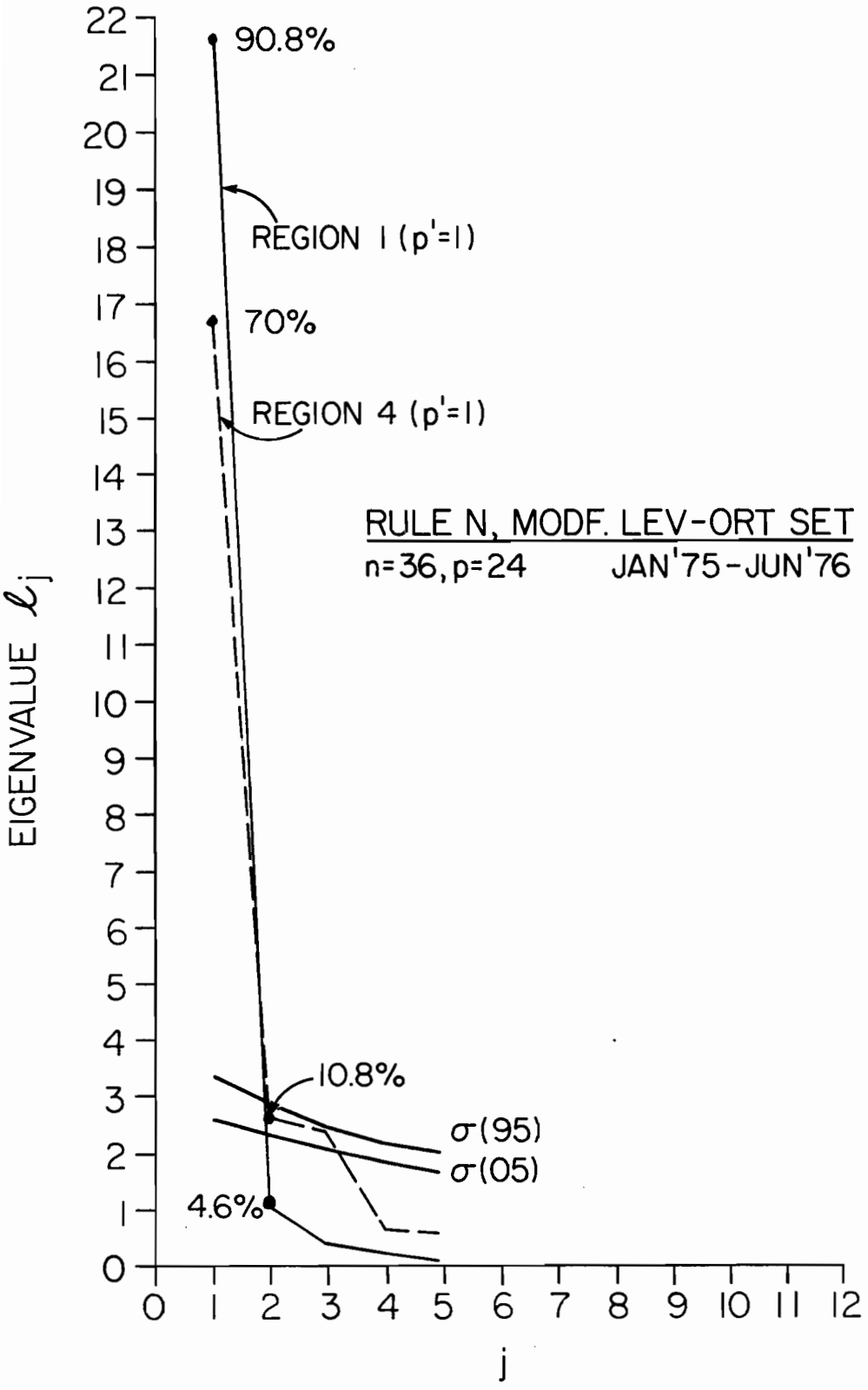
90.8%
REGION 1 (p'=1)
70%
REGION 4 (p'=1)
RULE N, MODF. LEV-ORT SET
n=36, p=24 JAN'75-JUN'76
10.8%
σ(95)
σ(05)
4.6%
EIGENVALUE ℓ_j
j
0 1 2 3 4 5 6 7 8 9 10 11 12
0 1 2 3 4 5 6 7 8 9 10 11 12 13 14 15 16 17 18 19 20 21 22

Fig. 6.2

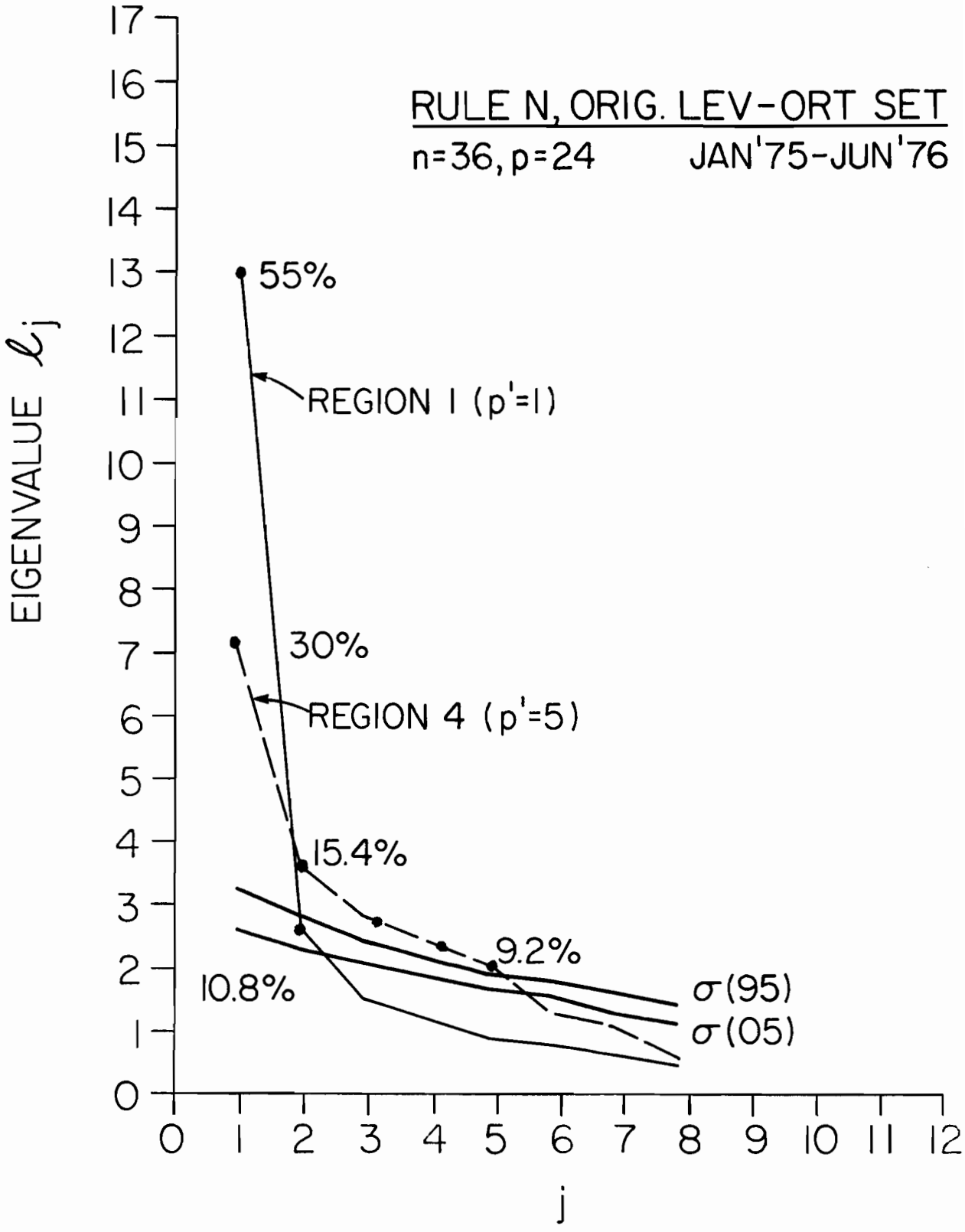
RULE N, ORIG. LEV-ORT SET
n=36, p=24 JAN'75-JUN'76
EIGENVALUE ℓ_j
55%
REGION 1 (p'=1)
30%
REGION 4 (p'=5)
15.4%
9.2%
10.8%
σ(95)
σ(05)
j
0 1 2 3 4 5 6 7 8 9 10 11 12
0 1 2 3 4 5 6 7 8 9 10 11 12 13 14 15 16 17

Fig. 6.3

Fig. 6.3, over region 1, the first eigenvalue of original L-O has only 55% of the variance with the remaining eigenvalues comparatively larger and tending toward simulating random structure. This is particularly pronounced in region 4, where, despite the fact that 5 eigenvalues are significant, the eigenvalue curve is becoming more like that of a random process (see Fig. 4.3 for Liu vs. original L-O, region 4).

B. Canonic Rotation Angles

In Appendix C of DIT(III) we developed the theory of canonic rotation angles θ_j of two data sets, and we shall apply it here to the three data sets: Liu, modified L-O, and original L-O. In Fig. 6.4 we have plotted the size-ordered canonic rotation angles for Liu vs. original Lev-Ort and Liu vs. modified Lev-Ort, for region 1.

Recall that these angles θ_j give a collective measure of the distance between $\underline{E}$ and $\underline{F}$ frames (and hence the spatial patterns) of the two data sets being intercompared. Thus, if e.g., $\underline{D}$ = Liu, $\underline{M}$ = original L-O, are the two $n \times p = 36 \times 24$ data sets with $\underline{E}$ and $\underline{F}$ frames, respectively, then for $\ell = p/2 = 12$.

$$\frac{1}{p} \|\underline{E} - \underline{F}\|^2 = \text{ORIEN}(\underline{E},\underline{F}) = \frac{2}{\ell} \sum_{j=1}^{\ell} (1 - \cos \theta_j) \qquad (6.1)$$

If the frames $\underline{E},\underline{F}$ are coincident, then $\theta_j = 0$, $j = 1,\cdots,\ell$, and the distance $\|\underline{E}-\underline{F}\|$ between them is zero. Moreover, if $(\underline{E}_1,\underline{F}_1)$ are the $\underline{E},\underline{F}$ frames of two data sets $\underline{D}_1,\underline{M}_1$, whose spatial patterns are relatively close compared to $(\underline{E}_2,\underline{F}_2)$ of data sets $\underline{D}_2,\underline{M}_2$, then we would expect the size-ordered sequence of θ_j's for the first pair $(\underline{D}_1,\underline{M}_1)$ to be on the whole smaller than the θ_j's for

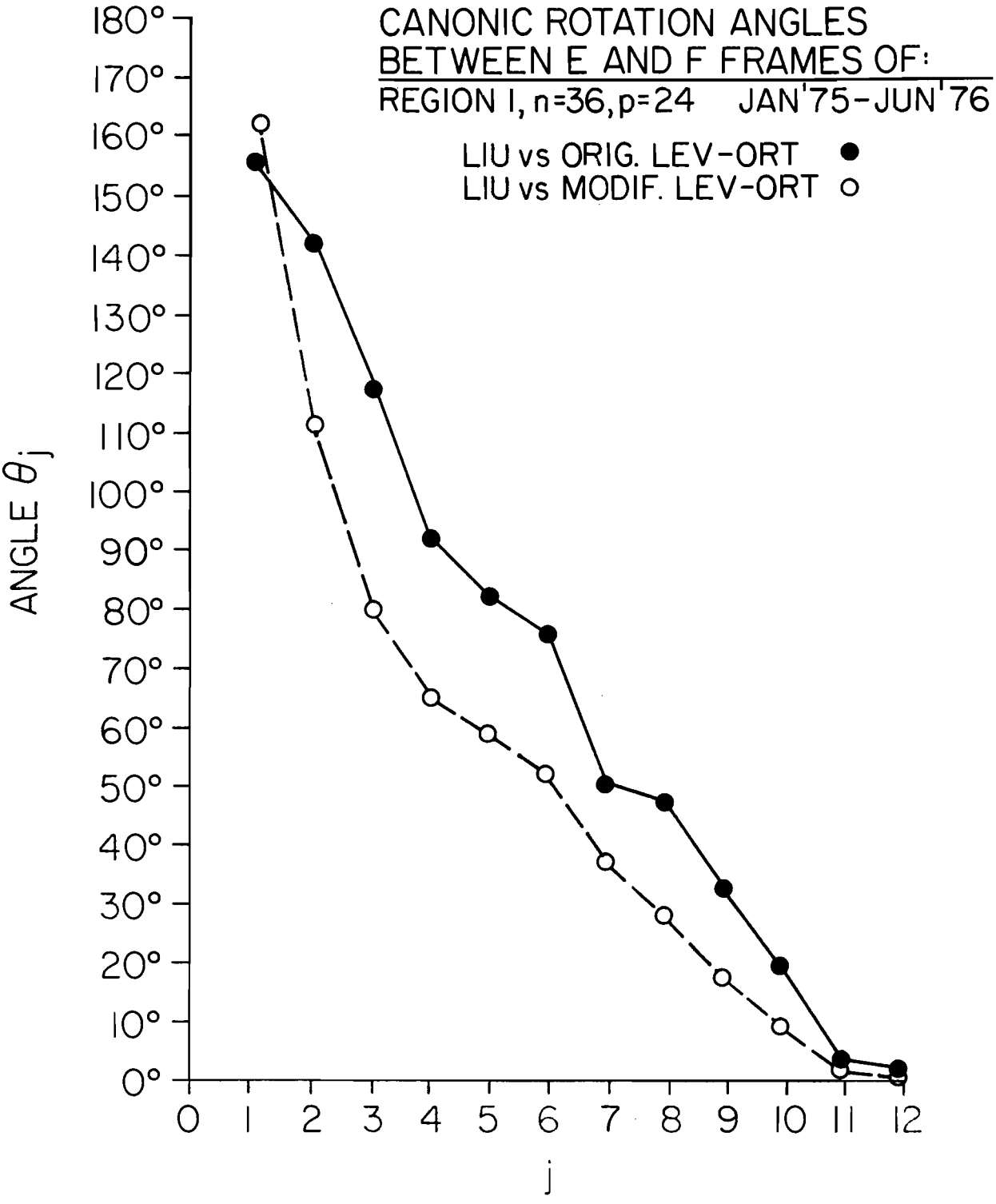
CANONIC ROTATION ANGLES
BETWEEN E AND F FRAMES OF:
REGION I, n=36, p=24 JAN'75-JUN'76
LIU vs ORIG. LEV-ORT
LIU vs MODIF. LEV-ORT
ANGLE θ_j
180°
170°
160°
150°
140°
130°
120°
110°
100°
90°
80°
70°
60°
50°
40°
30°
20°
10°
0°
0 1 2 3 4 5 6 7 8 9 10 11 12
j

Fig. 6.4

$(\underline{D}_2,\underline{M}_2)$. We have this situation in Fig. 6.4, where the size-ordered θ_j's for Liu vs. modified Lev-Ort are generally smaller than those of Liu vs. original Lev-Ort. This leads us in still another way (cf. Fig. 4.4) to the conclusion that the spatial pattern of Liu and modified Lev-Ort are closer than those of Liu and original Lev-Ort. Putting this more simply: the Liu pattern not only looks more like that of modified Lev-Ort than original Lev-Ort, but this visual fact is borne out by the objective Tercile, Trinity, and Canonic Rotation Tests.

C. Canonic Correlation Angles

In Appendix D of DIT(III) we developed the theory of canonic correlation angles ψ_j of two data sets, and we shall apply it here to the present three data sets. These angles give a collective measure of the distance between the $\underline{A}'$ and $\underline{B}'$ frames (and hence the temporal evolution) of any two data sets being intercompared. Thus

$$\frac{1}{p}\,\|\underline{A}'-\underline{B}'\|^2 = \mathrm{COREL}(\underline{A}',\underline{B}') = \frac{2}{p}\sum_{j=1}^{p}(1-\cos\psi_j) \qquad (6.2)$$

In the present case of n = 36, p = 24, on the basis of (D6.9) in DIT(III), we expect p-max[0, 2p - (n-1)] = 24 - 13 = 11 non zero canonic correlation angles. These are plotted in order of decreasing size in Fig. 6.5 for the data set pairs shown. We find the Liu set closer to the modified Lev-Ort set than to the original Lev-Ort set, as regards temporal evolution. This may be verified by inspection, using (6.2), for if the ψ_j decrease, so does $\mathrm{COREL}(\underline{A}',\underline{B}')$. We repeated the θ_j and ψ_j comparisons over region 2 and came to the same conclusions as above, now for region 2. The relevant plots are shown in Figs. 6.6, 6.7. Similar plots can be made for regions 3, 4.

CANONIC CORRELATION ANGLES
BETWEEN A' AND B' FRAMES OF:
REGION I, n=36, p=24 JAN'75-JUN'76
LIU vs ORIG. LEV-ORT
LIU vs MODIF. LEV-ORT
ANGLE ψ_j
90°
80°
70°
60°
50°
40°
30°
20°
10°
0°
0 1 2 3 4 5 6 7 8 9 10 11 12
j

Fig. 6.5

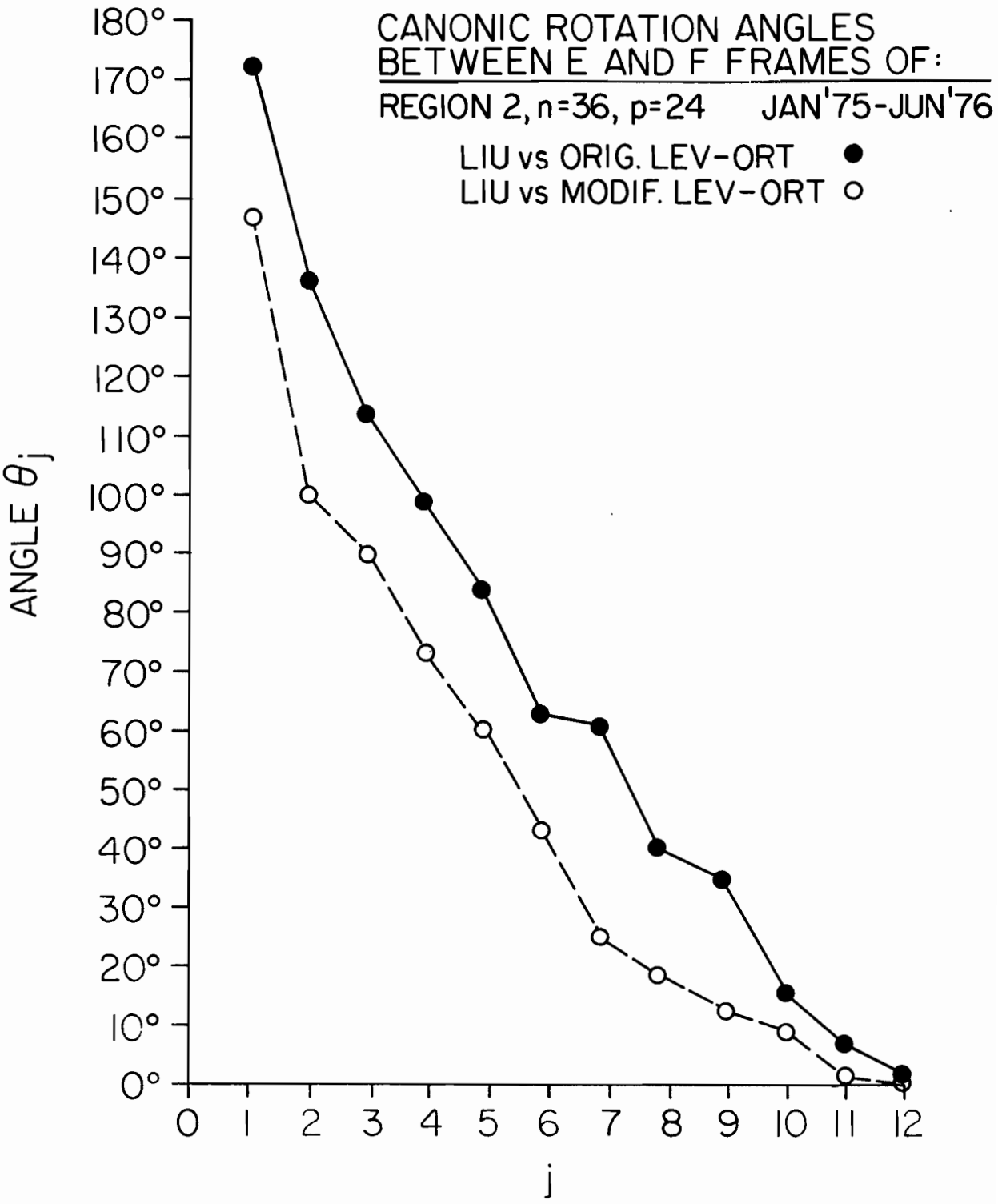
CANONIC ROTATION ANGLES
BETWEEN E AND F FRAMES OF:
REGION 2, n=36, p=24 JAN'75-JUN'76
LIU vs ORIG. LEV-ORT
LIU vs MODIF. LEV-ORT
ANGLE θ_j
180°
170°
160°
150°
140°
130°
120°
110°
100°
90°
80°
70°
60°
50°
40°
30°
20°
10°
0°
0 1 2 3 4 5 6 7 8 9 10 11 12
j

Fig. 6.6

CANONIC CORRELATION ANGLES
BETWEEN A' AND B' FRAMES OF:
REGION 2, n=36, p=24 JAN'75-JUN'76
LIU vs ORIG. LEV-ORT
LIU vs MODIF. LEV-ORT
ANGLE ψ_j
90°
80°
70°
60°
50°
40°
30°
20°
10°
0°
0 1 2 3 4 5 6 7 8 9 10 11 12
j

Fig. 6.7

We expect θ_j and ψ_j intercomparisons to be potentially useful indicators of spatial and temporal distances, between ($\underline{E}$,$\underline{F}$) and ($\underline{A}'$,$\underline{B}'$) frames, respectively. It would be interesting to apply the IOP and EOP of DIT(II) to (individual) θ_j and ψ_j values, ordered in decreasing size. The Liu set is potentially large enough to allow an IOP (Ideal Observation Procedure) resulting in useful distributions of the individual θ_j and ψ_j. Some novel principal component selection rules should be forthcoming from these considerations and their variants. For, by ordering the θ_j and ψ_j in decreasing size, just as we now do for eigenvalues, we can find the $\sigma(05)$, $\sigma(95)$ values for each θ_j,ψ_j. These would serve as bounds for the θ_j,ψ_j coming from two data sets to be intercompared, and thereby allow decisions as to statistical significance of the θ_j and ψ_j.

D. Spatial Correlation Tests

By way of contrast to the $\underline{E}$,$\underline{F}$ and $\underline{A}'$,$\underline{B}'$ intercomparisons of the preceding paragraph, we now use the correlation statistic to measure the closeness of the vectors $\underline{e}_j$ and $\underline{f}_j$ in $\underline{E}$ and $\underline{F}$, respectively. In Table 6.1 below, for Liu vs. modified Lev-Ort, over region 1, we list $r_j = \underline{e}_j^T \underline{f}_j$ for $j = 1,\cdots,24$ and the associated equivalent student-t measure*

$$t_j = \frac{r_j}{(1-r_j^2)^{\frac{1}{2}}} (p-2)^{\frac{1}{2}} \qquad (6.3)$$

---

* There may be some question over our choosing not to center the components of $\underline{e}_j,\underline{f}_j$ on their sample averages prior to forming r_j. The reader may wish to calculate his own version of Table 6.1 this way. We have chosen the present route, being guided by the derivation of the distribution of r_j given in Appendix E of DIT(III).

Here Liu = $\underline{D}$ and modified Lev-Ort = $\underline{M}$. Hence the $\underline{E}$ and $\underline{F}$ frames have the vectors $\underline{E} = \{\underline{e}_1 \cdots \underline{e}_p\}$, $\underline{F} = \{\underline{f}_1 \cdots \underline{f}_p\}$, $p = 24$. The 5% critical value for t is 1.72 for $p = 24$. From Table 6.1 we see that a considerable number of paired vectors $\underline{e}_j, \underline{f}_j$ in these frames are significantly close. The first three pairs $\underline{e}_j, \underline{f}_j$, $j = 1,2,3$, are very close, according to these measures of distance (recall $\|\underline{e}_j - \underline{f}_j\|^2 = 2(1 - \underline{e}_j^T \underline{f}_j)$), and we list their values in schematic form in Table 6.2 with their components arranged correctly in space over region 1. We have sketched in the contour lines suggested by these values. Thus, vectors $\underline{e}_1, \underline{f}_1$ are visually very close in pattern as are also vectors $\underline{e}_2, \underline{f}_2$ in the second pair of diagrams. The third pair of diagrams for $\underline{e}_3, \underline{f}_3$ are not visually close, but according to Table 6.1, $r_3 = \underline{e}_3^T \underline{f}_3 = .693$ and $t_3 = 4.504$ which is significant on the 5% level. This poor visual match is therefore somewhat belied by the significant t_3 value. The reader should at this point recall our comments on the unreliable nature of the correlation statistic in high-dimensional comparisons (DIT(III), §4).

E. Temporal Correlation Tests

For completeness, we include Table 6.3 below. The first two pairs of vectors $(\underline{\alpha}_1, \underline{\beta}_1)$ and $(\underline{\alpha}_2, \underline{\beta}_2)$ (recall Appendix B, DIT(III)) are highly significant according to the statistic: $r_j = \underline{\alpha}_j^T \underline{\beta}_j$, $j = 1, \cdots, 24$, used in (6.3) with "p" replaced by "n" and now $n = 36$. The 5% critical value for t is 1.69 for $n = 36$.

There are other significant pairs of $\underline{\alpha}_j, \underline{\beta}_j$ according to the test, but we keep in mind the observations on Table 6.2, made above. On the whole, rather than correlations, we would tend to trust Tercile Pattern Tests and displays of the kind in Figs. 6.4, 6.5, 6.6 (along with tests based on canonic direction angles*) to inform us whether two vectors or vector frames are significantly close or not.

---

* See §7, DIT(III), for research problems in these areas.

Table 6.1

Correlations Between Column Vectors $\underline{e}_j, \underline{f}_j$ of $\underline{E}, \underline{F}$ Frames Belonging to Liu and Modified Lev-Ort Sets over Region 1 (of Fig. 4.1) January 1975 - June 1976

j	r_j	t_j
1	.996	54.748
2	.971	18.968
3	.693	4.504
4	.522	2.869
5	.841	7.298
6	.824	6.832
7	.767	5.601
8	.778	5.806
9	.254	1.232
10	.208	1.000
11	.130	.614
12	.198	.949
13	.635	3.856
14	.185	.885
15	.480	2.568
16	.224	1.078
17	.617	3.673
18	.259	1.257
19	.145	.690
20	-.100	-.471
21	.576	3.309
22	.386	1.960
23	.202	.969
24	.947	13.874

Table 6.2

Visual Intercomparisons of $\underline{e}_j, \underline{f}_j$ of $\underline{E}, \underline{F}$ Frames Belonging to Liu and Modified Lev-Ort Sets Over Regions 1 (Fig. 4.1)

January 1975 - June 1976

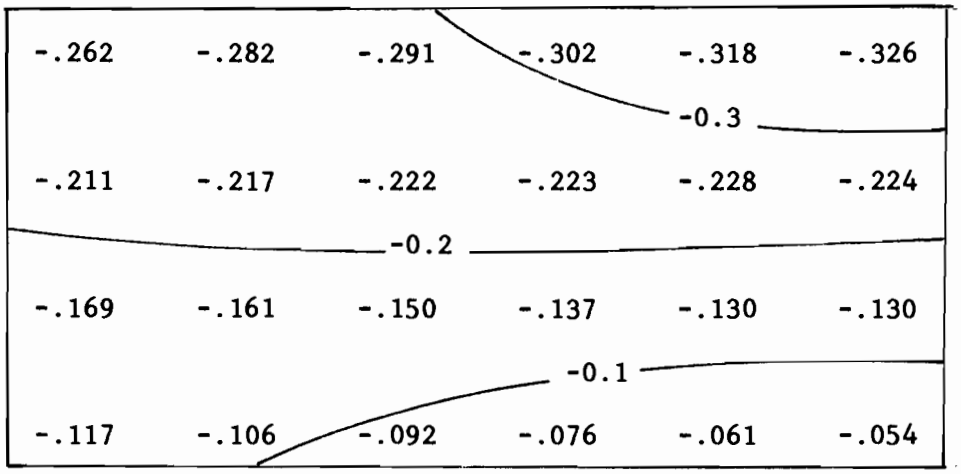

$\underline{e}_1$ (Liu)

Region 1

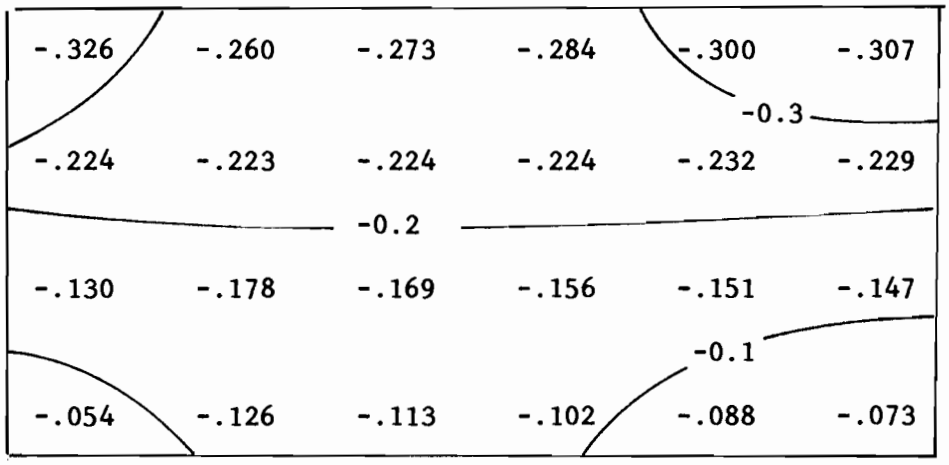

$\underline{f}_1$ (modified Lev-Ort)

Table 6.2 (Continued)

$\underline{e}_2$ (Liu)

Region 1

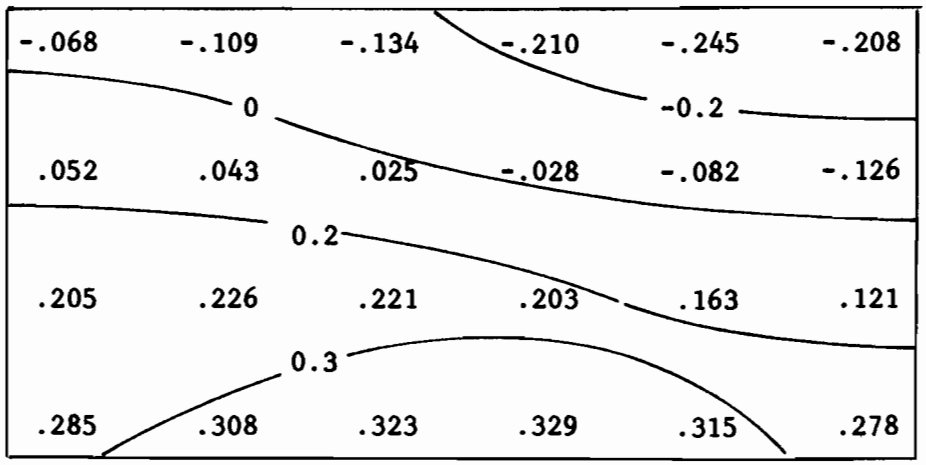

$\underline{f}_2$ (modified Lev-Ort)

Table 6.2 (Continued)

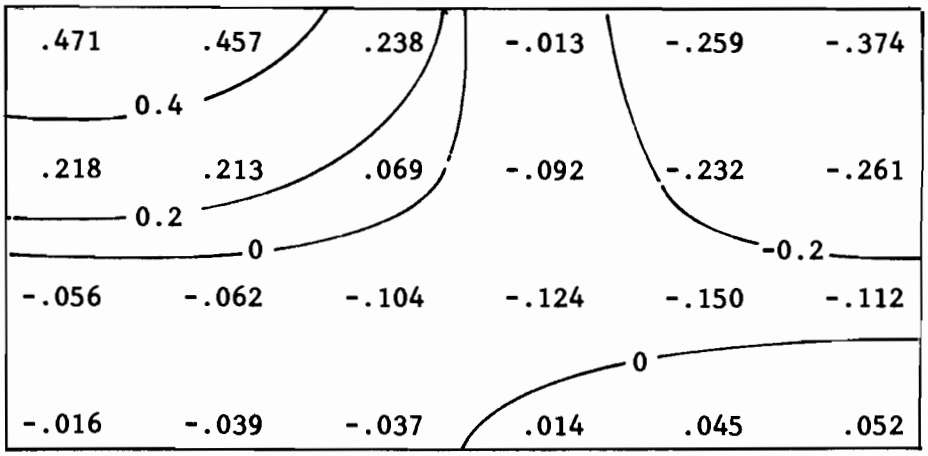

$\underline{e}_3$ (Liu)

Region 1

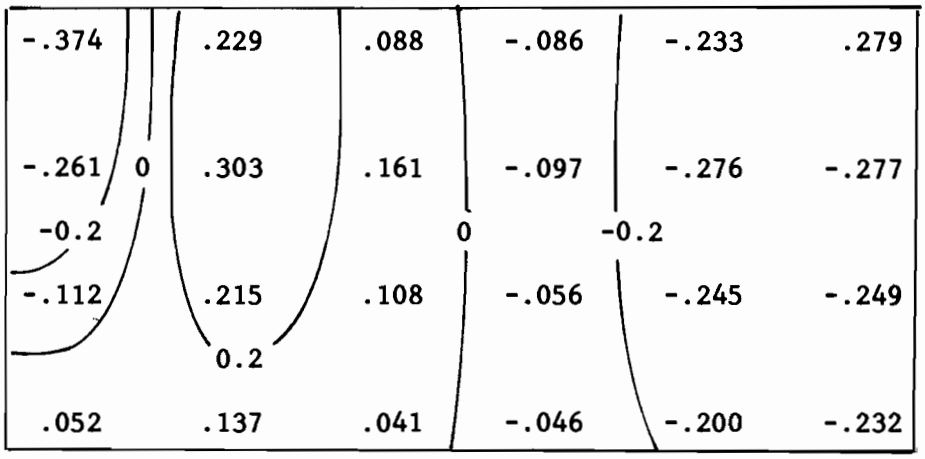

$\underline{f}_3$ (modified Lev-Ort)

Table 6.3

Correlation Between Column Vectors $\underline{\alpha}_j, \underline{\beta}_j$, of $\underline{A}', \underline{B}'$ Frames
Belonging to Liu and Modified Lev-Ort Sets Over Region 1 (of Fig. 4.1)
January 1975 - June 1976

j	r_j	t_j
1	.988	37.895
2	.933	15.120
3	.551	3.848
4	.523	3.579
5	.817	8.261
6	.803	7.853
7	.633	4.772
8	.704	5.778
9	.347	2.155
10	.171	1.015
11	.143	.844
12	.106	.619
13	.594	4.303
14	.071	.416
15	.287	1.746
16	.164	.968
17	.196	1.167
18	.327	2.015
19	.022	.127
20	-.199	-1.187
21	.545	3.790
22	.038	.223
23	.088	.514
24	.315	1.932

7. S-Phase and T-Phase Tests Applied to Liu, Modified L-O, and Original L-O Sets

The purpose of the S-phase test (cf. DIT(III)) is to help us decide whether the eigenframes $\underline{E},\underline{F}$ of two data sets $\underline{D},\underline{M}$, respectively, are significantly close or distant. The T-phase test does the same for the principal-component frames $\underline{A}',\underline{B}'$ of $\underline{D},\underline{M}$, respectively. The tests constitute an attempt to go beyond the simple θ_j-comparisons and ψ_j-comparisons in Figs. 6.4, 6.5 and in Figs. 6.6, 6.7. For, in those comparisons, as informative as they are concerning the relative closeness of orthonormal frames, we are still left in suspense about the statistical significance of these impressions of closeness.* Moreover, the θ_j and ψ_j, being purely geometric constructs and having no a priori connection with the physical processes giving rise to $\underline{D}$ and $\underline{M}$, leave us with a missing link to reality, which should eventually be included in an intercomparison study. The S-phase and T-phase tests are but one attempt to remedy these two inadequacies in the pure θ_j and ψ_j comparison exercises of §6. We shall now apply the S-phase and T-phase tests to the three data sets of the present study.

A. S-phase Test

Let us return to the setting of Fig. 6.4, and recall that, on setting $\underline{D}$ = Liu, and $\underline{M}$ = modified Lev-Ort, we found the canonic rotation angles θ_j, $j = 1,\cdots,12$ between the $\underline{E}$ and $\underline{F}$ frames, respectively, of these data sets over region 1. This constitutes STAGE I of the S-phase test (§5, DIT(III)). STAGE II finds the reference distribution for canonic rotation angles by means of a Monte Carlo procedure. In Fig. 7.1 we show this reference distribution as

---

* However, some research in this area may introduce significance tests for individual angles θ_j,ψ_j. See, e.g., our comments at the close of §6C.

derived from the Liu data set. STAGE III produces the link between reality (values of the $\underline{D}$ set) and the canonic rotation angles. The result is displayed in Fig. 7.2. In STAGE III we choose $\alpha = 0.10$, $\bar{f}_a = 0.10$, and the significantly-close option. The $\bar{f}_a$ choice (via Fig. 7.1) fixes θ_a as 12.2°. This θ_a in turn (via Fig. 7.2) fixes p_a as 0.10. The p_a and α values are used in a binomial probability distribution (cf. (5.8), (5.9) DIT(III)) to determine the critical number a(close) of θ_j required in the interval $[0,\theta_a]$ to decide if $\underline{E}$ and $\underline{F}$ are significantly close. It turns out that a(close) = 4. Therefore, to declare $\underline{E},\underline{F}$ significantly close, we need 5 or more θ_j in $[0,\theta_a]$ = [0, 12.2°]. By Fig. 6.4, the Liu vs. modified Lev-Ort curve has three angles (1.1°, 3.4°, 10.3°) in this interval. Hence we cannot declare that $\underline{E},\underline{F}$ are with confidence 90% significantly close. On this basis we conclude that the spatial patterns of the Liu and modified Lev-Ort data sets over region 1 are not significantly close.

If we choose instead the significantly-distant option, then with the same choice of $\alpha = 0.10$ and $\bar{f}_a = 0.10$, we find the critical value a(distant) (via (5.8), (5.10), DIT(III)) to be a(distant) = 1. The three angles in [0, 12.2°] noted above exceed this value. On this basis, we cannot conclude with confidence 90% that the spatial patterns of the Liu and modified Lev-Ort sets are significantly distant. In this sense, then, the sets are decided to be close in spatial pattern. If we relax α to $\alpha = 0.20$, and keep $\bar{f}_a = 0.10$, then a(distant) = 3, and now with these angles in [0, 12.2°], we can reject H_o and say the frames are significantly distant with confidence 80%.

These various conclusions suggest that the $\underline{E}$ and $\underline{F}$ frames of Liu and modified Lev-Ort subtend a borderline distance: neither very close or very distant in the view of the S-Phase test. Using the experience gained in §5C of DIT(III) (see, in particular, Table 5.1 there), we now repeat the S-phase

$\bar{f}(\theta)$ CURVE FOR LIU DATA SET, N=36, P=24
REGION I JANUARY 1975-JUNE 1976
FOR USE WITH S-PHASE TEST

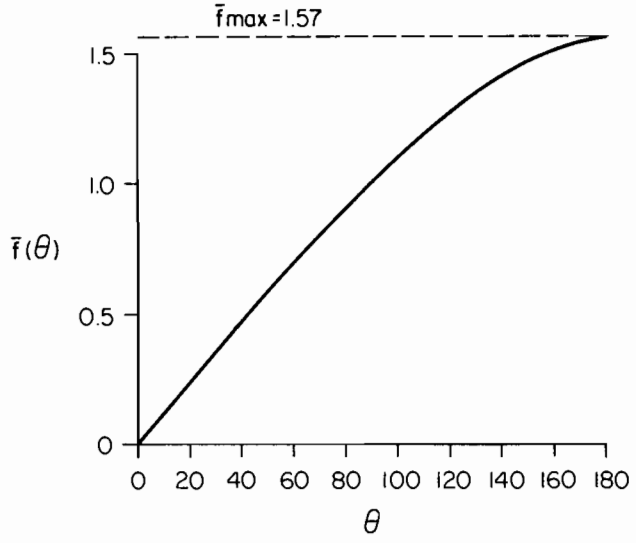

CUMULATIVE DISTRIBUTION FUNCTION FOR POOLED RANDOM CANONIC ROTATION ANGLES, N=36, P=24 (WITH MINIMUM ORIEN CONDITION)
FOR USE WITH S-PHASE TEST

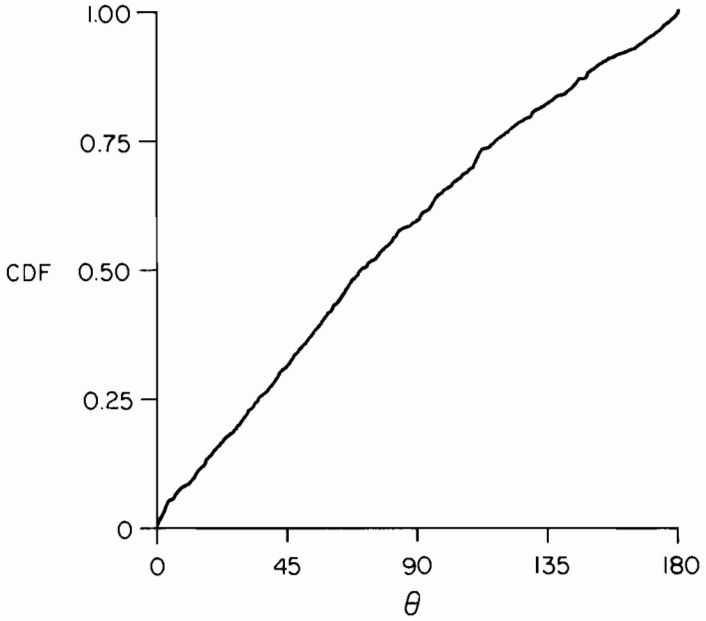

Fig. 7.1

Fig. 7.2

Table 7.1
S-Phase Tests, Liu vs. Modified Lev-Ort, Region 1
$\alpha = 0.10$, $n = 36$, $p = 24$ January 1975 - June 1976

$\bar{f}_a$	a(close)	θ_a	number of θ_j in $[0,\theta_a]$ (Fig. 6.4)	Decision on: significantly close option
0.10	4	12.2°	3	Accept H_o
0.20	5	25.3°	4	Accept H_o
0.30	6	39.7°	6	Accept H_o
0.40	8	54.1°	7	Accept H_o
0.50	9	68.5°	9	Accept H_o

test for several values of $\bar{f}_a$, using the significantly-close option. The results are in Table 7.1 above.

From this collection of decisions we see that two of them (for $\bar{f}_a = 0.30$, 0.50) are very near misses, i.e., we almost rejected H_o (that the original data sets $\underline{D},\underline{M}$ of the two frames $\underline{E},\underline{F}$, are drawn from the same population as in STAGE II). The others are also near misses. From this we would conclude that (for $\alpha = 0.10$) the $\underline{E}$ and $\underline{F}$ frames are borderline close. By examining the θ_j curve for Liu vs. *original* Lev-Ort in Fig. 6.4 and counting the number of θ_j in $[0,\theta_a]$ we see that the "misses" are now definitely wider than in the Liu vs. modified Lev-Ort case, i.e., we are further from the decision of significantly close spatial patterns for this pair of sets.

In sum, then, while the $\underline{E},\underline{F}$ frames of Liu and modified Lev-Ort cannot be rigorously declared significantly close on the 90% confidence level, using the S-phase test, they are nearly so, in the context of Table 7.1.

B. T-Phase Test

Returning to the setting of Fig. 6.5, with $\underline{D}$ = Liu and $\underline{M}$ = modified Lev-Ort, we find the canonic correlation angles ψ_j, $j = 1,\cdots,24$ between the

$\underline{A}'$,$\underline{B}'$ frames, respectively, of these data sets on region 1. This constitutes STAGE I of the T-phase test (§6, DIT(III)). STAGES II, III find the reference distributions for θ_j, ψ_j, and connect temporal rotations of Liu's set with its field changes (we shall not show these here). For STAGE IV we set $\bar{f}_a = 0.10$, $\alpha = 0.10$ and choose the significantly-close option. This fixes $\theta_a = 11.8°$ and in turn $p_a = .076$. From this, we find a(close) = 3, and $\psi_a = 26.6°$. Looking at Fig. 6.5, we see that for Liu vs. modified Lev-Ort, there are 4 angles in $[0,\psi_a] = [0, 26.6°]$, and so we declare the $\underline{A}'$,$\underline{B}'$ frames significantly close with confidence 90%. On the other hand, the Liu vs. original Lev-Ort curve in Fig. 6.5 has only 2 angles in [0, 26.6°] and we cannot declare the $\underline{A}'$,$\underline{B}'$ frames for this pair significantly close.

In sum, the T-phase test declares the $\underline{A}'$,$\underline{B}'$ frames of the Liu vs. modified Lev-Ort sets significantly close on the 90% confidence level.

8. Conclusions

We shall state some conclusions of the present case study, and then some conclusions in general, reached during the work of the present series on Data Intercomparison Theory.

A. Our final conclusion about the effects of the various operations in Liu's objective analysis scheme are represented succinctly in Tables 5.1, 5.2: Table 5.1 says that the *average SST value of the Liu SST data set* over its domain will not be significantly affected by removing, in part or in all, the various novel operations in Liu's scheme. Table 5.2 says that the removal of the SST-gradient sensitive and data weight features of Liu's scheme does not significantly affect the *variance of the Liu SST data set* over its domain.

However, dropping the particular smoothing operators in Liu's scheme (as summarized in Table 2.1) induces *significant changes* (increases) *in the variance of Liu's SST data set* over its domain. These changes amount to about 0.5° to 0.6°C (Table 5.3). Various other tests in this work corroborate these conclusions (tercile tests of §4; SITES and SPRED tests (via APP) of §5; applications of Rule N, canonic rotation angles, canonic correlation angles in §6; and S- and T-phase tests in §7).

B. The data intercomparison tests studied and introduced in DIT(I) - DIT(V) have been examined in various artificial and real data settings and have been found to be useful and occasionally powerful adjuncts to the classical intercomparison tests (student-t, correlation, T^2, M/b, etc.). The applications of the new tests to the Liu data sets have shown them illuminating differences and similarities from several novel perspectives. All these new tests are offered here in a tentative way, with further study and experimentation with them expected to be made as they are applied to a wider range of data settings. The further research problems they suggest (cf. §7, DIT(III), e.g.) should eventually yield a battery of data intercomparison tools for use in processing the huge data sets arising in modern climate diagnosis and prediction research.

9. References

DIT(I): Minimal Spanning Tree Tests for Location and Scale Differences.

DIT(II): Trinity Statistics for Location, Spread and Pattern Differences.

DIT(III): S-Phase and T-Phase Tests for Spatial Pattern and Temporal Evolution Differences.

DIT(IV): Tercile Tests for Location, Spread and Pattern Differences.

DIT(V): Case Study: Effects of Objective Analysis on a Tropical Pacific Sea Surface Temperature Set.

Cressman, G. (1959) "An Operational Objective Analysis System," Mon. Wea. Rev. 87, 367.

Levitus, S., A. Oort (1977) "Global Analysis of Oceanographic Data," Bull. Am. Met. Soc. 58, 1270.

Liu, C-T. (1982) Analysis of Tropical Pacific Sea Surface Temperatures for 1975 to 1980. Tech. memo. ERL PMEL-34, Pacific Marine Environmental Laboratory, Seattle, Wash.

Preisendorfer, R.W., F.W. Zwiers, T.P. Barnett (1981) Foundations of Principal Component Selections Rules. SIO Ref. 81-4. Scripps Institution of Oceanography, La Jolla, Cal.

Weare, B.C., A.R. Navato, R.E. Newell (1976) "Empirical Orthogonal Analysis of Pacific Sea Surface Temperature," J. Phys. Ocn. 6, 671.

Appendix A

Exposition of Cressman-Liu Objective Analysis Scheme

1. Introduction

The data intercomparison procedures of the main text above dwell on systematic variations of an objective analysis scheme devised by Cho-Teng Liu (1982). In order to choose these systematic variations for our various purposes, we have studied the structure of Liu's scheme to identify essential elements he has added to the Cressman (1959) and Levitus-Oort (1977) analyses to obtain his present scheme. Knowledge of the various steps in Liu's method of analysis lets us follow the physical actions involved in these scheme-variations and also allows us to physically understand the statistically significant differences (if any) among the resultant sets. The variations of Liu's scheme resulted in the "modified Lev-Ort," and "original Lev-Ort" data sets. These were obtained by applying the varied schemes to the basic raw data set assembled by Liu (1982). The resultant differences among the three data sets have been discussed at length in the main text. Here we assemble the key logical elements of Liu's objective analysis scheme.

2. Outline of Study

We consider in turn the following fifteen main topics:

Domain

Domain Borders

Grid

Data Field on Rack (Irregular Domain)

Climate Field on Grid (Regular Domain)

Extension of Climate Field from Grid to Domain

Gradients of Climate Field

APPENDIX A

Reach Function

Outlier Function

Data Weight Function

Influence Function (Station to Node)

Interpolation Function (Node to Station)

Diffusion Box

Smoothing Cross and Laplacian

The Iterative Transformations

3. Domain

The *domain* D in this study is a rectangular parametric region that provides a geometric simulation of a portion of the sea surface and adjacent land regions (see Fig. A3.1). Points in the domain D are specified by ordered pairs of *latitude* and *longitude* angles x, y, respectively. Thus the domain D is defined as:

$$D \equiv \{(x,y): x_o \leqq x \leqq x_1, y_o \leqq y \leqq y_1\} \qquad (A3.1)$$

The limits x_o, x_1 and y_o, y_1 of D are fixed at the outset and a regular network of lines of longitude (constant x) and latitude (constant y) of fixed separations Δx, Δy respectively, is chosen, so that $a \equiv [x_1 - x_o]/\Delta x$, $b \equiv [y_1 - y_o]/\Delta y$ are positive integers. The intersections of the regular network of longitude and latitude lines are called *nodes*, and each is located at points of the form $(x_o + i\Delta x, y_o + j\Delta y)$ in D, $i = 0,\cdots,a$; $j = 0,\cdots,b$. The set of nodes of D will be denoted by "N." There are (a+1)(b+1) nodes in N. Any point (x,y) in D has a unique *address* $A(x,y) \equiv (i,j)$ where i,j are those

DATA DOMAIN AND ASSOCIATED CONCEPTS

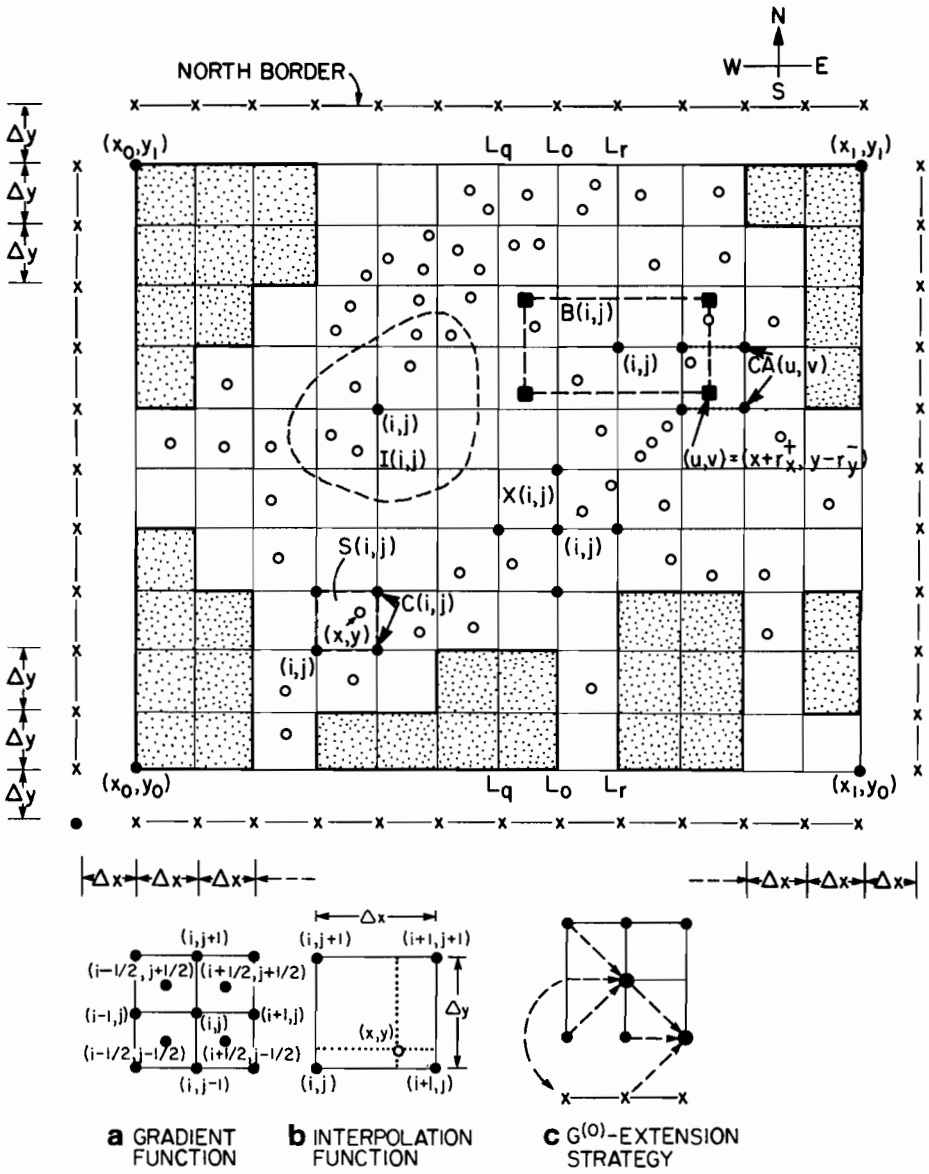

a GRADIENT FUNCTION **b** INTERPOLATION FUNCTION **c** $G^{(0)}$-EXTENSION STRATEGY

LEGEND

(i,j)	=NODE ●
(x,y)	=STATION ○
A(x,y)	=(i,j) ADDRESS OF STATION (x,y)
B(i,j)	=BOX AT (i,j) (4 NODES)
C(i,j)	=CELL AT (i,j) (4 NODES)
X(i,j)	=CROSS AT (i,j) (4 NODES)
S(i,j)	=SQUARE AT (i,j) (CONTINUUM)
I(i,j)	=INFLUENCE DOMAIN AT (i,j) (SEVERAL STATIONS)
CA(u,v)	=CELL FOR POINT (u,v) ■

Fig. A3.1

two integers in the ranges $0 \leqq i \leqq a$, $0 \leqq j \leqq b$, such that the remainders

$$x' \equiv x - (x_o + i\Delta x), \qquad y' \equiv y - (y_o + j\Delta y) \tag{A3.2}$$

satisfy $$0 \leqq x' < \Delta x \quad , \qquad 0 \leqq y' < \Delta y \tag{A3.3}$$

The *cell* C(i,j) *at* (i,j) is the set of four addresses:

$$C(i,j) = \{(i,j),\ (i+1,j),\ (i+1,j+1),\ (i,j+1)\} \tag{A3.4}$$

The *square* S(i,j) *with address* (i,j) is the subset of D of the form

$$S(i,j) = \{(x,y):\ A(x,y) = (i,j)\} \tag{A3.5}$$

We also say that: S(i,j) is the square of cell C(i,j). Let (x,y) be a point of D. Then A(x,y) = (i,j) is its address and C(A(x,y)) = C(i,j) ("CA(x,y)" for short) is the *cell at* A(x,y). In other words, each point (x,y) of D may be associated with a unique cell and in particular with a unique square-subset of D whose corners have the elements of the cell as its addresses. The *center* of S(i,j) is the point $(x_o + i\Delta x + \frac{1}{2}\Delta x,\ y_o + j\Delta y + \frac{1}{2}\Delta y)$. We give the center of S(i,j) the *half-integer address* $(i+\frac{1}{2},\ j+\frac{1}{2})$.

4. Domain Borders

The *north* and *south borders* of D are discrete sets of integer pairs

$$D_N \equiv \{(i,b+1):\ i = 0,\cdots,a\} \tag{A4.1}$$

$$D_S \equiv \{(i,-1):\ i = 0,\cdots,a\} \tag{A4.2}$$

The *east* and *west borders* of D are discrete sets of integer pairs:

$$D_E \equiv \{(a+1,j): \quad j = 0,\cdots,b\} \tag{A4.3}$$

$$D_W \equiv \{(-1,j): \quad j = 0,\cdots,b\} \tag{A4.4}$$

Thus D_N, e.g., is a set of addresses of points of the form $(x_o + i\Delta x, y_o + (b+1)\,\Delta y)$, $i = 0,\cdots,a$ just *north* of D, in the hypothesized latitude, longitude system of D.

5. Grid

A *grid* G of the domain D is a subset of the set N of nodes of D. The grid is specified by designating those nodes of D that are to belong to G. This may be done arithmetically by defining a membership function m(i,j) on the set of addresses of N. Thus m(i,j) = 1 if and only if $(x_o + i\Delta x, y_o + j\Delta x)$ is in G and m(i,j) = 0 if not. The choice of m(i,j) (i.e., G) is left to each researcher to make, as required by the objective analysis problem at hand.

6. Data Field on Rack (Irregular Domain)

The raw data comes as values D(x,y) of a field (such as sea surface temperature or sea level pressure) at points (x,y) of an irregularly-scattered subset of D. This subset of D we will call the *rack* R. The points of R are called *stations*. The object of the transformation theory in §17 below is to use the values of D(x,y) on R to determine a *function* d'(i,j) on the grid G. The result of the transformation is the required *objectively analyzed data set.*

Each point (x,y) of the rack R has a unique address A(x,y). By going systematically through R we can determine and list A(x,y) for all (x,y) in R. From this, we can list, conversely, all the (x,y) of R in each square S(i,j) of D. By making this systematic census of the elements of R in each square S(i,j), at the outset of an objective analysis, various operations (e.g., in construction of the influence domain I(i,j)) are greatly facilitated.

7. Climate Field on Grid

In the original Cressman (1959) scheme it was assumed that there is a climatology field $G^{(0)}(i,j)$ on the nodes $(x_o + i\Delta x, y_o + j\Delta y)$ of the grid G and also that $G^{(0)}$ $(i+\frac{1}{2}, j+\frac{1}{2})$ is given on the centers of each square S(i,j). It may be the case, however, that at the outset $G^{(0)}$ is not defined on all nodes of D. In the following section we outline how the extension of $G^{(0)}$ from G to N can be done.

8. Extension of Climate Field from Grid to Domain

In order to get the extension underway it is necessary to have $G^{(0)}$ defined on at least one line of longitude on which each node is both in G and N. Such a line is shown, e.g., as L_oL_o in Fig. A3.1. From this line we can march east and west of L_oL_o and fill in $G^{(0)}$ values as follows.

If L_rL_r with $r \geq 0$ is a line of longitude east of L_oL_o with points $(x_o + r\Delta x, y_o + j\Delta y)$ and $G^{(0)}$ is defined on L_rL_r, then we define $G^{(0)}$ on $L_{r+1}L_{r+1}$ via the rules:

Set:

(a) $G^{(0)}(r,-1) = G^{(0)}(r,1), \quad G^{(0)}(r,b+1) = G^{(0)}(r,b-1)$

(b) For every $j = 0,\cdots,b$ and r such that $0 \leqq r \leqq a$,

$$\begin{cases} \text{if } m(r+1,j) = 0, \text{ then } G^{(0)}(r+1,j) = \\ \qquad \tfrac{1}{2}G^{(0)}(r,j) + \tfrac{1}{4}[G^{(0)}(r,j+1) + G^{(0)}(r,j-1)] \\ \text{if } m(r+1,j) = 1, \text{ then go to node with address } (r+1,j+1) \end{cases}$$

A picture of this extension process is given in part (c) of Fig. A3.1. The figure depicts the grid near the southern border. The function $m(i,j)$ is defined in §5.

If L_qL_q is a line of longitude west of L_oL_o, with points of the form $(x_o + q\Delta x, y_o + j\Delta y)$ and $G^{(0)}$ is defined on L_qL_q, then we define $G^{(0)}$ on $L_{q-1}L_{q-1}$ via the rules:

(a) Set

$$G^{(0)}(q,-1) = G^{(0)}(q,1), \quad G^{(0)}(q,b+1) = G^{(0)}(q,b-1)$$

(b) For every $j = 0,\cdots,b$ and q such that $0 \leqq q \leqq a$,

$$\begin{cases} \text{if } m(q-1,j) = 0, \text{ then } G^{(0)}(q-1,j) = \\ \qquad \tfrac{1}{2}G^{(0)}(q,j) + \tfrac{1}{4}[G^{(0)}(q,j+1) + G^{(0)}(q,j-1)] \\ \text{if } m(q-1,j) = 1, \text{ then go to node with address } (q-1,j+1) \end{cases}$$

A picture of this extension process is obtained from part (c) of Fig. A3.1 by directing the drift of arrows in the figure toward the west. Observe that the

process of extension automatically extends $G^{(0)}$ to the four borders of D. The extension of $G^{(0)}$ to the centers of squares S(i,j) of D is made in precisely the same way by starting along some line of longitude through square centers at each of which $G^{(0)}$ is known. The result, if correctly done, should define $G^{(0)}$ also at the ***half-integer addresses of points between*** D and its four borders. (Part (a) of each of the extension rules above would then respectively extend $G^{(0)}$ at latitude level ½ to latitude level -½ at the southern border, and from the b-½ latitude level to the b+½ level at the northern border.)

9. Gradients of Climate Field

The gradients of the climate field are used in the influence function. For any node with address (i,j),

$$G_x^{(0)}(i,j) = \tfrac{1}{2}\left[\frac{G^{(0)}(i+\frac{1}{2},j+\frac{1}{2}) - G^{(0)}(i-\frac{1}{2},j+\frac{1}{2})}{\Delta x} + \frac{G^{(0)}(i+\frac{1}{2},j-\frac{1}{2}) - G^{(0)}(i-\frac{1}{2},j-\frac{1}{2})}{\Delta x} \right] \tag{A9.1}$$

and

$$G_y^{(0)}(i,j) = \tfrac{1}{2}\left[\frac{G^{(0)}(i+\frac{1}{2},j+\frac{1}{2}) - G^{(0)}(i+\frac{1}{2},j-\frac{1}{2})}{\Delta y} + \frac{G^{(0)}(i-\frac{1}{2},j+\frac{1}{2}) - G^{(0)}(i-\frac{1}{2},j-\frac{1}{2})}{\Delta y} \right] \tag{A9.2}$$

for $i = 0,\cdots,a$; $j = 0,\cdots,b$.

A picture of this process is given in part (a) of Fig. A3.1. Thus there are two estimates of $G_x^{(0)}(i,j)$ at (i,j) which are averaged. Similarly for the y derivative.

10. Reach Functions

The *reach functions* form integral parts of the influence function. We define

$$R_x(i,j) \equiv \frac{b_x}{c_x + d_x|G_x^{(0)}(i,j)|} \tag{A10.1}$$

$$R_y(i,j) \equiv \frac{b_y}{c_y + d_y|G_y^{(0)}(i,j)|} \tag{A10.2}$$

for $i = 0,\cdots,a$; $j = 0,\cdots,b$.

The quantities b_x, c_x, b_y, c_y are dimensionless parameters. d_x, d_y have units degrees (longitude or latitude) per degree (Celsius). In Liu (1982), we have $b_x = b_y = 3$, or 4, depending on iteration index (as on §17, below). Also $c_x = c_y = 0.5$ with $d_x = d_y = 2$ for all iterations.

11. Outlier Function

When constructing the correction field, below, it will be necessary to remove data values D(x,y) that differ markedly from the current field estimate at (x,y), namely $E^{(r)}(x,y)$. For this purpose we introduce the Heaviside function H(z|c), which here will be the *outlier function:*

$$H(z|c) = \begin{cases} 0 \text{ if } z \geq c \\ \\ 1 \text{ if } z < c \end{cases} \tag{A11.1}$$

The cutoff values c are specified in advance, and are listed in §17 below.

12. Data Weight Functions

Liu defines two functions f_a, f_c to be used with his particular data source sets. These will be parts of the influence function. We have:

$$f_a(x,y) = \left\{ \begin{array}{l} 1 \text{ if datum is drawn from SPOT} \\ 2 \text{ if datum is drawn from EPOCS} \\ 4 \text{ if datum is drawn from BATHY} \\ 8 \text{ if datum is drawn from XBT} \end{array} \right\} \text{ at } (x,y) \text{ in } D \qquad \text{(A12.1)}$$

$$f_c(x,y) = \frac{4}{2 + |D(x,y) - E^{(0)}(x,y)|} \text{ , at } (x,y) \text{ on } D \qquad \text{(A12.2)}$$

Here $\underline{E}^{(0)}(x,y)$ is the interpolated climate field from a cell to an internal point (x,y) in the cell's square; it will be defined below in §17 as part of the iteration process. Throughout all iterations, (A12.2) continues to use $E^{(0)}(x,y)$.

13. Influence Function (Station to Node)

Let (i,j) be the address of a grid node. The *influence domain* $I(i,j)$ for (i,j) is the subset of points (x,y) of the rack R for which

$$\rho(i,j|x,y) \leqq 1, \qquad \text{(A13.1)}$$

where

$$\rho(i,j|x,y) = \left[\frac{(x-i\Delta x)^2}{R_x^2(i,j)} + \frac{(y-j\Delta y)^2}{R_y^2(i,j)} \right]^{\frac{1}{2}} \qquad \text{(A13.2)}$$

for $i = 0,\cdots,a$; $j = 0,\cdots,b$, and $x_o \leqq x \leqq x_1$, $y_o \leqq y \leqq y_1$

The *primary influence function* is defined as

$$W'(i,j|x,y) \equiv \begin{cases} f_a(x,y)\ f_c(x,y)\ \exp\{-4\rho^2(i,j|x,y)\}, & \rho(i,j|x,y) \leqq 1 \\ 0, & \rho(i,j|x,y) > 1 \end{cases} \tag{A13.3}$$

The *normalized influence function* is then

$$W(i,j|x,y) = W'(i,j|x,y) / \sum_{(x,y)\varepsilon I(i,j)} W'(i,j|x,y) \tag{A13.4}$$

for $i = 0,\cdots,a$; $j = 0,\cdots,b$ and $(x,y)\varepsilon I(i,j)$

It is at this point where the constructions, suggested in §6 for the influence domain, are greatly facilitated, especially when the numbers of points in R and N are relatively great. Thus, at each (i,j) one can pre-determine the (x,y) of the rack R in I(i,j) and hence relatively simply find the denominator in (A13.4).

14. Interpolation Function (Node to Station)

Given a point (x,y) in D, to this point we associate a containing square S(i,j). When the field values of some field G(i,j) are defined on the corner nodes of the square, then these values may be used, via interpolation, to assign a value E(x,y) to the point (x,y) in D, using

$$E(x,y) \equiv \sum_{(i,j)\varepsilon CA(x,y)} \alpha(x,y|i,j)G(i,j) \tag{A14.1}$$

Here CA(x,y) is the four-address cell at A(x,y), as indicated in (b) of Fig. A3.1. That is,

$$CA(x,y) = \{(i,j),\ (i+1,j),\ (i+1,j+1),\ (i,j+1)\} \qquad (A14.2)$$

Moreover,

$$\alpha(x,y|i,j) = \left[\frac{y - j\Delta y}{\Delta y}\right]\left[\frac{x - i\Delta x}{\Delta x}\right] \qquad (A14.3)$$

$$\alpha(x,y|i+1,j) = \left[\frac{y - j\Delta y}{\Delta y}\right]\left[\frac{(i+1)\Delta x - x}{\Delta x}\right] \qquad (A14.4)$$

$$\alpha(x,y|i+1,j+1) = \left[\frac{(j+1)\Delta y - y}{\Delta y}\right]\left[\frac{(i+1)\Delta x - x}{\Delta x}\right] \qquad (A14.5)$$

$$\alpha(x,y|i,j+1) = \left[\frac{(j+1)\Delta y - y}{\Delta y}\right]\left[\frac{x - i\Delta x}{\Delta x}\right] \qquad (A14.6)$$

so that

$$\sum_{(i,j)\varepsilon CA(x,y)} \alpha(x,y|i,j) = 1 \qquad (A14.7)$$

The *interpolation function* $\alpha(x,y|i,j)$ may be used to carry information from nodes $(x_o + i\Delta x,\ y_o + j\Delta y)$ in the grid to points (x,y) in the rack.

15. Diffusion Box

There may be some subregions of domain D of the data field D(x,y) over which the above interpolation cannot initially be done. For example, there may be points (x,y) in R such that the function D(x,y) is not initially defined in or around the vicinity of the points with addresses CA(x,y). By repeated applications of the diffusion activity defined below, however, we can eventually smoothly spread the D(x,y) field to all nodes of domain D. Let (i,j) be the address of some node of the grid. Then for every function H(u,v) defined on D we may assign a new function M(i,j) on the grid such that

$$M(i,j) = \tfrac{1}{4} \sum_{(u,v)\varepsilon B(i,j)} H(u,v) \qquad \text{(A15.1)}$$

for $i = 0,\cdots,a$; $j = 0,\cdots,b$.

Here B(i,j) is the set of four points of the form (u,v) in D defined as:

$$B(i,j) = \{(x + r_x^+, y + r_y^+), (x - r_x^-, y + r_y^+),$$

$$(x - r_x^-, y - r_y^-), (x + r_x^+, y - r_y^-)\} \qquad \text{(A15.2)}$$

where $x = x_o + i\Delta x$, $y = y_o + j\Delta y$, and where, using (A10.1), (A10.2),

$$\begin{aligned} r_x^+ &= \min [R_x(i,j), (a-i)\Delta x] \\ r_y^+ &= \min [R_y(i,j), (b-j)\Delta y] \\ r_x^- &= \min [R_x(i,j), i\Delta x] \\ r_y^- &= \min [R_y(i,j), j\Delta y] \end{aligned} \qquad \text{(A15.3)}$$

We call B(i,j) the *box* with address (i,j).

A picture of B(i,j) is given in the main diagram of Fig. A3.1. The coordinates (u,v) of the southeast corner of B(i,j) are shown. For grid points deep inside D, B(i,j) is simply the four corner points of a rectangle centered on (i,j) and of sides with lengths $2R_x(i,j)$, $2R_y(i,j)$ in longitude and latitude angle measure. If the node $(x_o + i\Delta x, y_o + j\Delta y)$ is near enough to the boundary of D, then (A15.3) will direct the computer to take as a corner of B(i,j) the nearest grid node in the appropriate east-west or north-south direction from (i,j). In this way, the four points of the box B(i,j) will always be within D, and occasionally within N.

16. Smoothing Cross and Laplacian

Another smoothing operation akin to (A15.1) operates on field values $F(k,\ell)$, about a node of N with address (i,j), to yield a new function G(i,j):

$$G(i,j) = \tfrac{1}{4} \sum_{(k,\ell)\varepsilon X(i,j)} F(k,\ell) \qquad \text{(A16.1)}$$

where

$$X(i,j) = \{(i+1,j),\ (i,j+1),\ (i-1,j),\ (i,j-1)\} \qquad \text{(A16.2)}$$

and $i = 0,\cdots,a;\ j = 0,\cdots,b$.

Also, for any function G(i,j) on the nodes of N we define a new function $\Delta G(i,j)$:

$$\Delta G(i,j) \equiv \tfrac{1}{4} \left[\sum_{(k,\ell)\varepsilon X(i,j)} G(k,\ell) \right] - G(i,j) \qquad \text{(A16.3)}$$

A picture of the *cross* X(i,j) is shown in the main diagram of Fig. 3.1. The transformation from G(i,j) to the function $\Delta G(i,j)$ is a discrete version of the Laplacian operator, an efficient smoother of data.

17. The Iterative Transformations

The core of the Cressman-Liu objective analysis procedure rests in the following sequence of five operations. One starts with iteration index r = 0 and uses the given climate field $G^{(0)}(i,j)$ on the set N of nodes of D, along with the given data field D(x,y) on the rack R. Then, in the order shown, the operations below are performed at each $(x_o + i\Delta x,\ y_o + j\Delta y)$ of N and (x,y) of R.

Grid to Rack interpolator:

$$E^{(r)}(x,y) \equiv \tfrac{1}{4} \sum_{(i,j)\ \varepsilon\ CA(x,y)} \alpha(x,y|i,j)\ G^{(r)}(i,j) \qquad \text{(A17.1)}$$

Corrector on Grid:

$$C^{(r)}(i,j) \equiv \sum_{(x,y)\ \varepsilon\ I(i,j)} W(i,j|x,y)\ H(D(x,y) - E^{(r)}(x,y)|c^{(r)})(D(x,y) - E^{(r)}(x,y)) \qquad \text{(A17.2)}$$

Diffuser-Smoother:

$$M^{(r)}(i,j) \equiv \tfrac{1}{4} \sum_{(u,v)\ \varepsilon\ B(i,j)} [\tfrac{1}{4} \sum_{(k,\ell)\ \varepsilon\ CA(u,v)} \alpha(u,v|k,\ell)\ G^{(r)}(k,\ell)] \qquad \text{(A17.3)}$$

Updater:

$$F^{(r+1)}(i,j) \equiv \tfrac{1}{2} \{(G^{(r)}(i,j) + C^{(r)}(i,j)) + M^{(r)}(i,j)\} \qquad \text{(A17.4)}$$

Curvature-corrector:

$$G^{(r+1)}(i,j) \equiv \tfrac{1}{4} \sum_{(k,\ell)\ \varepsilon\ X(i,j)} F^{(r+1)}(k,\ell) - \Delta G^{(0)}(i,j) \qquad \text{(A17.5)}$$

The activity in (A17.3) may be followed using the pictures of B(i,j) and CA(u,v) in Fig. A3.1. In (A17.2), the cutoff levels $c^{(r)}$ of (A11.1) along with the $b^{(r)}$ ($= b_x^{(r)} = b_y^{(r)}$) values of (A10.1), (A10.2), as used by Liu, are as defined in the table below

r	$b^{(r)}$	$c^{(r)}$
0	4	7°C
1	4	5
2	4	4
3	4	3
4	3	3
5	3	2.5
6	3	2.5

(A17.6)

APPENDIX A

In Liu (1982) seven iteration values of r were used r = 0,···,6, and the final G-values are given by the cross smoother in (A16.1):

$$d'(i,j) \equiv G^{(8)}(i,j) \equiv \tfrac{1}{4} \sum_{(k,\ell)\ \varepsilon\ X(i,j)} G^{(7)}(k,\ell) \qquad \text{(A17.7)}$$

for i = 0,···,a; j = 0,···,b.

NOAA ERL technical reports, technical memoranda, and data reports published by authors at Pacific Marine Environmental Laboratory in Seattle, Washington, are listed below. Microfiche copies are available from the USDOC, National Technical Information Service (NTIS), 5285 Port Royal Road, Springfield, Virginia 22161 (703-487-4650). Hard copies of some of these publications are available from the ERL Library in Boulder, Colorado (303-497-3271). Hard copies of some of the technical reports are sold by the Superintendent of Documents, U.S. Government Printing Office, Washington, D.C. 20402 (202-275-9251).

NOAA Technical Report Series

ERL82-POL1 Naugler, Frederic P. (1968)
Bathymetry of a region (PORL-421-2) North of the Hawaiian Ridge, pre-NTIS.

ERL93-POL2 Grim, Paul J. (1968)
Seamap deep-sea channel, Jan. 1969, 2 824 50 060, pre-NTIS.

ERL118-POL3 Le Mehaute, Bernard (1969)
An introduction to hydrodynamics and water waves, 2 vols. 725 pp.
NTIS: PB192 065, PB192 066.

ERL146-POL4 Rea, David K. (1970)
Bathymetry and magnetics of a region (POL-421-3) 29° to 35°N, 155° to 165°W.
NTIS: COM-71-00173.

ERL191-POL5 Reed, R.K. (1970)
Results from some parachute drogue measurements in the central North Pacific Ocean, 1961-1962, 9 pp.
NTIS: COM-71-50020.

ERL214-POL6 Lucas, William H. (1971)
Gravity anomalies and their relation to major tectonic features in the North Central Pacific, 19 pp.
NTIS: COM-71-50409.

ERL229-POL7 Halpern, David (1972)
Current meter observations in Massachusetts Bay, 36 pp.
NTIS: AD-745 465.

ERL230-POL8 Lucas, William H. (1972)
South Pacific RP-7-SU-71 Pago Pago to Callao to Seattle.
NTIS: COM-72-50454.

ERL231-POL9 Halpern, David (1972)
Description of an experimental investigation on the the response of the upper ocean to variable winds, 51 pp.
NTIS: COM-72-50452.

ERL232-POL10 Stevens, H. R., Jr. (1972)
RP-1-OC-71 Northeast Pacific geophysical survey, 91 pp.
NTIS: COM-72-50677.

ERL234-POL11 Lucas, William H. (1972)
Juan de Fuca Ridge and Sovanco fracture zone.
RP-5-OC-71, 39 pp.
NTIS: COM-72-50854.

ERL240-POL12 Halpern, David (1972)
Wind recorder, current meter and thermistor chain measurements in tbe northeast Pacific-August/September 1971, 37 pp.
NTIS: COM-73-50107.

ERL247-POL13 Cannon, G. A. and Norman P. Laird (1972)
Observations of currents and water properties in Puget Sound, 1972, 42 pp.
NTIS: COM-73-50402.

ERL252-POL14 Cannon, G. A., N. P. Laird, T. V. Ryan (1973)
Currents observed in Juan de Fuca submarine canyon and vicinity, 1971. 57 pp.
NTIS: COM-73-50401.

ERL258-POL15 Lucas, William H., and Richard R. Uhlhorn (1973)
Bathymetric and magnetic data from the northeast Pacific 40° to 58°N, 125° to 160°W. 9 pp.
NTIS: COM-73-50577.

ERL259-POL16 Ryan, T. V., N. P. Laird, G. A. Cannon (1973)
RP-6-OC-71 Data Report: Oceanographic conditions off the Washington coast, October-November 1971, 43 pp.
NTIS: COM-73-50922

ERL260-POL17 Cannon, Glenn A. (1973)
Observations of currents in Puget Sound, 1970, 77 pp.
NTIS: COM-73-50666/9.

ERL261-POL18 Stevens, H. R. Jr., (1973)
RP-1-OC-70 Southeast Pacific geophysical survey, 60 pp.
NTIS: not available.

ERL271-POL19 Reed, Ronald K., and David Halpern (1973)
STD observations in the northeast Pacific, September-October 1972, 58 pp.
NTIS: COM-73-50923/4.

ERL292-PMEL20 Reed, R. K. (1973)
Distribution and variation of physical properties along the SEAMAP standard section, 16 pp.
NTIS: COM-74-50334/3.

ERL323-PMEL21 Erickson, B. H. (1975)
Nazca plate program of the international decade of ocean exploration--OCEANOGRAPHER Cruise-RP 2-OC-73, 78 pp.
NTIS: COM-7540911/6.

ERL325-PMEL22 Halpern, D., J. M. Helseth, J. R. Holbrook, and R. M. Reynolds (1975)
Surface wave height measurements made near the Oregon coast during August 1972, and July and August 1973, 168 pp.
NTIS: COM-75-10900/9.

ERL327-PMEL23 Laird, N. P., and Jerry A. Galt (1975)
Observations of currents and water properties in Puget Sound, 1973, 141 pp.
NTIS: COM-73-50666/9.

ERL333-PMEL24 Schumacher, J. D., and R. M. Reynolds (1975)
STD, current meter, and drogue observations in Rosario Strait, January-Marcb 1974, 212 pp.
NTIS: COM-75-11391/0.

ERL339-PMEL25 Galt, J. A. (1975)
Development of a simplified diagnostic model for interpretation of oceanographic data.
NTIS: PB-247 357/7.

ERL352-PMEL26 Reed, R. K., (1975)
An evaluation of formulas for estimating clear-sky insolation over the ocean, 25 pp.
NTIS: PB-253 055/8.

ERL384-PMEL27 Garwood, Roland (1977)
A general model of tbe ocean mixed layer using a two-component turbulent kinetic energy budget with mean turbulent field closure, 81 pp.
NTIS: PB-265 434/1.

ERL390-PMEL28 Hayes, S. P., and W. Zenk (1977)
Observations of the Antarctic Polar Front by a moored array during FDRAKE-76, 47 pp.
NTIS: PB-281 460/6.

ERL390-PMEL29 Hayes, S. P., and W. Zenk (1977)
Observations of the Antarctic Polar Front by a moored array during FDRAKE-76, 49 pp.
NTIS: PB-281 460/6.

ERL403-PMEL30 Chester, Alexander J. (1978)
Microzooplankton in tbe surface waters of the Strait of Juan de Fuca, 26 pp.
NTIS: PB 297233/AS.

ERL404-PMEL31 Schumacher, J. D., R. Sillcox, D. Dreves, and R. D. Muench (1978)
Winter circulation and hydrography over the continental shelf of the northwest Gulf of Alaska, 16 pp.
NTIS: PB 296 914/AS.

ERL407-PMEL32 Overland, J. E., M. H. Hitchman, and Y. J. Han (1979)
A regional surface wind model for mountainous coastal areas, 34 pp.
NTIS: PB 80 146 152.

ERL412-PMEL33 Holbrook, J. R., R. D. Muench, D. G. Kachel, and C. Wright (1980)
Circulation in the Strait of Juan de Fuca: Recent oceanographic observations in the Eastern Basin, 42 pp.
NTIS: PB 81-135352.

ERL415-PMEL34 Feely, R. A., and G. J. Massoth (1982)
Sources, composition, and transport of suspended particulate matter in lower Cook Inlet and northern Shelikof Strait, Alaska, 28 pp.
NTIS: PB 82-193263

ERL417-PMEL35 Baker, E. T. (1982)
Suspended particulate matter in Elliott Bay, 44 pp.
NTIS: PB 82-246943.

ERL419-PMEL36 Pease, C. J., S. A. Schoenberg, J. E. Overland (1982)
A climatology of the Bering Sea and its relation to sea ice extent, 29 pp.
NTIS: not yet available.

ERL422-PMEL37 Reed, R. K. (1982)
Energy fluxes over the eastern tropical Pacific Ocean, 1979-1982, 15 pp.
NTIS: PB 83 138305

NOAA Data Report Series

ERL PMEL-1 Mangum, L., N. N. Soreide, B. D. Davies, B. D. Spell, and S. P. Hayes (1980)
CTD/O_2 measurements during the equatorial Pacific Ocean climate study (EPOCS) in 1979, 643 pp.
NTIS: PB 81 211203.

ERL PMEL-2 Katz, C. N., and J. D. Cline (1980)
Low molecular weight hydrocarbon concentrations (C_1-C_4), Alaskan continental shelf, 1975-1979, 328 pp.
NTIS: PB 82 154211.

ERL PMEL-3 Taft, B. A., and P. Kovala (1981)
Vertical sections of temperature, salinity, thermosteric anomaly, and zonal geostrophic velocity from NORPAX shuttle experiment, part 1, 98 pp.
NTIS: PB 82 163106.

ERL PMEL-4 Pullen, P. E., and H. Michael Byrne (1982)
Hydrographic measurements during the 1978 cooperative Soviet-American tsunami expedition, 168 pp.
NTIS: not yet available.

ERL PMEL-5 Taft, B.A., P. Kovala, and A. Cantos-Figuerola (1982)
Vertical sections of temperature, salinity, thermosteric anomaly and zonal geostrophic velocity from NORPAX Shuttle Experiment--Part 2, 94 pp.
NTIS:

ERL PMEL-6 Katz, C.N., J.D. Cline, and K. Kelly-Hansen (1982)
Dissolved methane concentrations in the southeastern Bering Sea, 1980 and 1981, 194 pp.
NTIS:

NOAA Technical Memorandum Series

ERL PMEL-1 Sokolowski, T. J. and G. R. Miller (1968)
Deep sea release mechanism, Joint Tsunami Research Effort, pre-NTIS.

ERL PMEL-2 Halpern, David (1972)
STD observations in the northeast Pacific near 47°N, 128°W (August/September 1971), 28 pp.
NTIS: COM-72-10839.

ERL PMEL-3 Reynolds, R. Michael and Bernard Walter, Jr. (1975)
Current meter measurements in the Gulf of Alaska--Part I: Results from NEGOA moorings 60, 61, 62A, 28 pp.
NTIS: PB-247 922/8.

ERL PMEL-4 Tracy, Dan E. (1975)
STD and current meter observations in the north San Juan Islands, October 1973.
NTIS: PB-248 825/2.

ERL PMEL-5 Holbrook, James R. (1975)
STD measurements off Washington and Vancouver Island during September 1973.
NTIS: PB-249 918/4.

ERL PMEL-6 Charnell, R. L. and G. A. Krancus (1976)
A processing system for Aandersa current meter data, 53 pp.
NTIS: PB-259 589/0.

ERL PMEL-7 Mofjeld, Harold O. and Dennis Mayer (1976)
Formulas used to analyze wind-driven currents as first-order autoregressive processes, 22 pp.
NTIS: PB-262 463/3.

ERL PMEL-8 Reed, R. K. (1976)
An evaluation of cloud factors for estimating insolation over the ocean, 23 pp.
NTIS: PB-264 174/4.

ERL PMEL-9 Nakamura, A. I. and R. R. Harvey (1977)
Versatile release timer for free vehicle instrumentation over the ocean, 21 pp.
NTIS: PB 270321/AS.

ERL PMEL-10 Holbrook, James R. and David Hslpern (1977)
A compilation of wind, current, bottom pressure, and STD/CTD measurements in the northeast Gulf of Alaska, February-May 1975.
NTIS: PB 270285.

ERL PMEL-11 Nakamura, A. I. and R. R. Harvey (1978)
Conversion from film to magnetic cassette recording for the Geodyne 102 current meter, 17 pp.
NTIS: PB-283 349/9.

ERL PMEL-12 Hayes, S. P., J. Glenn, N. Soreide (1978)
A shallow water pressure-temperature gage (PTG): Design, calibration, and operation, 35 pp.
NTIS: PB 286 754/7.

ERL PMEL-13 Schumacher, J. D., R. K. Reed, M. Grigsby, D. Dreves (1979)
Circulation and hydrography near Kodiak Island, September to November 1977, 52 pp.
NTIS: PB 297421/AS.

ERL PMEL-14 Pashinski, D. J., and R. L. Charnell (1979)
Recovery record for surface drift cards released in the Puget Sound-Strait of Juan de Fuca system during calendar years 1976-1977, 32 pp.
NTIS: PB 299047/AS.

ERL PMEL-15 Han, Y.-J. and J. A. Galt (1979)
A numerical investigation of the Bering Sea circulation using a linear homogeneous model, 40 pp.
NTIS: PB 299884/AS.

ERL PMEL-16 Loomis, Harold G. (1979)
A primer on tsunamis written for boaters in Hawaii, 10 pp.
NTIS: PB80-161003.

ERL PMEL-17 Muench, R. D. and J. D. Schumacher (1980);
(Hayes, Charnell, Lagerloef, and Pearson, contributors)
Some observations of physical oceanographic conditions on the northeast Gulf of Alaska continental shelf, 90 pp.
NTIS: PB81-102584.

ERL PMEL-18 Gordon, Howard R., ed. (1980)
Ocean remote sensing using lasers, 205 pp.
NTIS: PB80-223282.

ERL PMEL-19 Cardone, V. J. (1980)
Case studies of four severe Gulf of Alaska storms, 58 pp.
NTIS: PB81-102519.

ERL PMEL-20 Overland, J. E., R. A. Brown, and C. D. Mobley (1980)
METLIB--A program library for calculating and plotting marine boundary layer wind fields, 82 pp.
NTIS: PB81-141038.

ERL PMEL-21 Salo, S. A., C. H. Pease, and R. W. Lindsay (1980)
Physical environment of the eastern Bering Sea, March 1979, 127 pp.
NTIS: PB81-148496.

ERL PMEL-22 Muench, R. D., and J. D. Schumacher (1980)
Physical oceanographic and meteorological conditions in the northwest Gulf of Alaska, 147 pp.
NTIS: PB81-199473.

ERL PMEL-23 Wright, Cathleen (1980)
Observations in the Alaskan Stream during 1980, 34 pp.
NTIS: PB81-207441.

ERL PMEL-24 McNutt, L. (1980)
Ice conditions in the eastern Bering Sea from NOAA and LANDSAT imagery: Winter conditions 1974, 1976, 1977, 1979, 179 pp.
NTIS: PB81-220188.

ERL PMEL-25 Wright, C., and R. K. Reed (1980)
Comparison of ocean and island rainfall in the tropical South Pacific, Atlantic, and Indian Oceans, 17 pp.
NTIS: PB81-225401.

ERL PMEL-26 Katz, C. N. and J. D. Cline (1980)
Processes affecting distribution of low-molecular-weight aliphatic hydrocarbons in Cook Inlet, Alaska, 84 pp.
NTIS: not yet available.

ERL PMEL-27 Feely, R. A., G. J. Massoth, A. J. Paulson (1981)
Distribution and elemental composition of suspended matter in Alaskan coastal waters, 119 pp.
NTIS: PB82-124538.

ERL PMEL-28 Muench, R. D., J. D. Schumacher, and C. A. Pearson (1980)
Circulation in the lower Cook Inlet, Alaska, 26 pp.
NTIS: PB82-126418.

ERL PMEL-29 Pearson, C. A. (1981)
Guide to R2D2--Rapid retrieval data display, 148 pp.
NTIS: PB82-150384.

ERL PMEL-30 Hamilton, S. E., and J. D. Cline (1981)
Hydrocarbons associated with suspended matter in the Green River, Washington, 116 pp.
NTIS: PB82-148677.

ERL PMEL-31 Reynolds, R. M., S. A. Macklin, and T. R. Heister (1981)
Observations of South Alaskan coastal winds, 49 pp.
NTIS: PB82-164823.

ERL PMEL-32 Pease, C. H., and S. A. Salo (1981)
Drift characteristics of northeastern Bering Sea ice during 1980, 79 pp.
NTIS: PB 83 112466

ERL PMEL-33 Ikeda, Motoyoshi (1982)
Eddies detached from a jet crossing over a submarine ridge: A study using a simple numerical model, 38 pp.
NTIS: PB82-217563.

ERL PMEL-34 Liu, Cho-Teng (1982)
Tropical Pacific sea surface temperature measured by SEASAT microwave radiometer and by ships, 160 pp.
NTIS: not yet available.

ERL PMEL-35 Lindsay, R.W., and A.L. Comiskey (1982):
Surface and upper-air observations in the eastern Bering Sea, 90 pp.
NTIS: not yet available.

ERL PMEL-36 Preisendorfer, R., and C. E. Mobley (1982)
Climate forecast verifications off the U. S. mainland, 1974-1982, 225 pp.
NTIS: not yet available.